



RESEARCH PAPER



Garcinia cambogia attenuates adipogenesis by affecting CEBPB and SQSTM1/p62-mediated selective autophagic degradation of KLF3 through RPS6KA1 and STAT3 suppression

Joo-Hui Han ^{*}, Keun-Woo Jang, and Chang-Seon Myung ^{*}

Department of Pharmacology, College of Pharmacy, Chungnam National University, Daejeon, Republic of Korea

ABSTRACT

The overexpansion of adipose tissues leads to obesity and eventually results in metabolic disorders. *Garcinia cambogia* (*G. cambogia*) has been used as an antiobesity supplement. However, the molecular mechanisms underlying the effects of *G. cambogia* on cellular processes have yet to be fully understood. Here, we discovered that *G. cambogia* attenuated the expression of CEBPB (CCAAT/enhancer binding protein (C/EBP), beta), an important adipogenic factor, suppressing its transcription in differentiated cells. In addition, *G. cambogia* inhibited macroautophagic/autophagic flux by decreasing autophagy-related gene expression and autophagosome formation. Notably, *G. cambogia* markedly elevated the expression of KLF3 (Kruppel-like factor 3 (basic)), a negative regulator of adipogenesis, by reducing SQSTM1/p62-mediated selective autophagic degradation. Furthermore, increased KLF3 induced by *G. cambogia* interacted with CTBP2 (C-terminal binding protein 2) to form a transcriptional repressor complex and inhibited *Cebpa* and *Pparg* transcription. Importantly, we found that RPS6KA1 and STAT3 were involved in the *G. cambogia*-mediated regulation of CEBPB and autophagic flux. In an obese animal model, *G. cambogia* reduced high-fat diet (HFD)-induced obesity by suppressing epididymal and inguinal subcutaneous white adipose tissue mass and adipocyte size, which were attributed to the regulation of targets that had been consistently identified *in vitro*. These findings provide new insight into the mechanism of *G. cambogia*-mediated regulation of adipogenesis and suggest molecular links to therapeutic targets for the treatment of obesity.

Abbreviations: 3-MA: 3-methyladenine; ACTB: actin beta; ATG: autophagy-related; Baf: bafilomycin A₁; BECN1: beclin 1; CEBP: CCAAT/enhancer binding protein (C/EBP); CHX: cycloheximide; CREB: cAMP response element binding protein; CTBP: C-terminal binding protein; EGCG: (-)-epigallocatechin gallate; eWAT: epididymal white; *G. cambogia*: *Garcinia cambogia*; GFP: green fluorescent protein; H&E: hematoxylin and eosin; HFD: high-fat diet; iWAT: inguinal subcutaneous white; KLF: Kruppel-like factor; LAP: liver-enriched transcriptional activating proteins; MAP1LC3/LC3: microtubule-associated protein 1 light chain 3; ND: normal diet; PPARG: peroxisome proliferator activated receptor gamma; qPCR: quantitative real-time PCR; RFP: red fluorescent protein; RPS6KA1: ribosomal protein S6 kinase A1; siRNA: small-interfering RNA; SQSTM1/p62: sequestosome 1; STAT: signal transducer and activator of transcription; TEM: transmission electron microscopy

ARTICLE HISTORY

Received 2 October 2020
Revised 20 May 2021
Accepted 25 May 2021

KEYWORDS

Adipogenesis; autophagy; CEBPB; *Garcinia cambogia*; KLF3; obesity; RPS6KA1; SQSTM1/p62; STAT3

Introduction


Adipose tissue is not only a storage site of excess energy in the form of lipids but also an endocrine organ playing a central role in metabolic homeostasis [1,2]. The overexpansion of adipose tissue mass is a major driving force in obesity and related complications, such as type 2 diabetes, hyperlipidemia and atherosclerosis [3,4]. Thus, it is important to investigate the molecular mechanisms underlying adipogenesis to identify novel therapeutics for obesity and related metabolic disorders.

Adipogenesis involves several processes that are regulated by various adipogenic transcription factors, such as CEBPs (CCAAT/enhancer binding protein (C/EBP)s) and PPARG (peroxisome proliferator activated receptor gamma) [5,6]. CEBPs belong to a large family of basic leucine zipper

transcription factors, including A/α, B/β, G/γ, D/δ, E/ε and Z/ζ members [7]. Among these transcription factors, the levels of CEBPB and CEBPD are increased during early adipogenesis and then activate the expression of *Cebpa* and *Pparg* by binding to their promoters [8]. Since CEBPA and PPARG can mutually induce expression in a positive feedback loop and serve as pleiotropic transactivators of many adipocyte-specific genes [9,10], these two key transcription factors are delicately controlled by multiple positive and negative regulators, such as KLFs (Kruppel-like factors), WNT1 (wnt family member 1) and DLK1 (delta like non-canonical Notch ligand 1) [11–13]. Notably, KLF2 represses *Pparg* promoter activity by binding to the *Pparg2* promoter region [14], and KLF3 directly binds to the endogenous *Cebpa* promoter with corepressors, such as CTBP (C-terminal binding protein), and represses its activity

CONTACT Joo-Hui Han  han5621@cnu.ac.kr; Chang-Seon Myung  cm8r@cnu.ac.kr  Department of Pharmacology, College of Pharmacy, Chungnam National University, Daejeon, Republic of Korea

^{*}These correspondence contributed equally to this paper.

 Supplemental data for this article can be accessed [here](#).

© 2021 Informa UK Limited, trading as Taylor & Francis Group

and protein expression [15,16]. Therefore, controlling these regulators is important for initiating the expression of adipogenic transcription factors and triggering differentiation.

Autophagy is a cellular degradative process that maintains homeostasis, in which damaged organelles and cellular proteins are sequestered in autophagosomes that subsequently fuse with lysosomes for degradation and recycling [17]. *ATG* (autophagy related) genes and proteins are involved in the regulation of this process [18]. Of note, adipose tissues in obese patients and animal models exhibit elevated autophagy, but the mechanisms by which autophagy alters adipogenic factors are poorly understood [19,20]. Impaired autophagy by genetic deletion or pharmacological agents [21] has been associated with reduced adipose tissue mass [22] and improved insulin sensitivity [23]. Thus, it is of extreme importance to identify potent autophagy inhibitors and related molecular targets that specifically regulate adipogenesis.

Garcinia cambogia (*G. cambogia*), a fruit that is native to Southeast Asia, is now most commonly used as a weight-loss supplement [24–26]. There are many studies on the anti-obesity effect of *G. cambogia* extract in animal models [27,28]. Recently, we reported that *G. cambogia* extract suppressed adipogenic hormonal stimulation (differentiation medium)-mediated phosphorylation and nuclear translocation of RPS6KA1 (ribosomal protein S6 kinase A1) and STAT3 (signal transducer and activator of transcription 3) within 0–120 min, without affecting the upstream molecules, MAPK1 (mitogen-activated protein kinase 1)/ERK2 (extracellular signal-regulated kinase 2)-MAPK3/ERK1 and JAK2 (Janus kinase 2) [29,30], thus inhibited mitotic clonal expansion (MCE) in the early stage of adipocyte differentiation [31]. Despite these findings, the underlying mechanisms and interaction of target molecules through which *G. cambogia* extract regulates adipogenesis remain poorly understood.

In this study, we investigated the effects of *G. cambogia* extract on CEBPB and autophagy regulation in adipocytes. Our findings show the inhibitory effects of *G. cambogia* extract on *Cebpb* transcription and autophagic flux by suppressing the levels of autophagy-related genes and the formation of autophagosomes and autolysosomes through inhibiting RPS6KA1 and STAT3. Moreover, *G. cambogia* extract enhanced the expression of KLF3 by inhibiting SQSTM1/p62-mediated selective autophagic degradation, resulting in increasing the interaction of KLF3 with CTBP2 to form a transcriptional repressor complex. Additionally, the physiological impacts of the identified targets were corroborated in adipose tissues from obese mice.

Results

G. cambogia extract inhibits adipogenesis and potently affects 0–4 days of the early stage of adipocyte differentiation

We previously reported that *G. cambogia* extract (100, 200 and 300 µg/ml) had an inhibitory effect on lipid accumulation and did not affect cell viability for 72 h in 3T3-L1 preadipocytes using not only MTT [31] but also LDH release assays

(Fig. S1). In addition, adipogenic hormonal stimulation by MDI (DMEM containing 0.5 µM 3-isobutyl-1-methylxanthine [IBMX], 5 µM dexamethasone, 0.5 µg/ml insulin and 10% FBS) maximally induced RPS6KA1 and STAT3 phosphorylation at 15 min and 2 h in MDI-induced 3T3-L1 preadipocytes (differentiation started cells), and cotreatment with *G. cambogia* extract significantly inhibited phosphorylation of RPS6KA1 after 15 and 30 min and phosphorylation of STAT3 after 1 and 2 h of stimulation.

As shown in Figure 1A, *G. cambogia* extract dually attenuated RPS6KA1 and STAT3 phosphorylation in MDI-induced 3T3-L1 preadipocytes after 15 min or 2 h of stimulation, which was different from the effects of the specific signaling inhibitors, FMK (RPS6KA1 inhibitor) and stattic (STAT3 inhibitor). Since *G. cambogia* extract did not affect the phosphorylation of MAPK1/ERK2-MAPK3/ERK1 and JAK2, upstream molecules of RPS6KA1 and STAT3, in a previous study [31], we examined MAPK3/ERK1, one of the MAPK isoforms, and JAK2 kinase activities to clarify the mechanism by which *G. cambogia* extract regulates RPS6KA1 and STAT3. By using an *in vitro* kinase assay, we found that *G. cambogia* extract inhibited the kinase activity of MAPK3/ERK1 and JAK2 and consequently suppressed RPS6KA1 and STAT3 phosphorylation (Figure 1B). Furthermore, FMK and stattic inhibited the expression of CEBPA and PPARG, which are critical transcription factors in adipogenesis [32], and *G. cambogia* extract potently blocked the expression of two key factors in mature 3T3-L1 adipocytes (fully differentiated adipocytes) indicating that RPS6KA1 and STAT3 might regulate CEBPA and PPARG during adipogenesis (Figure 1C).

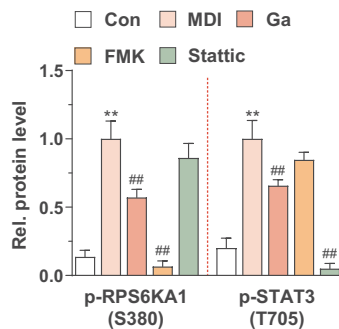
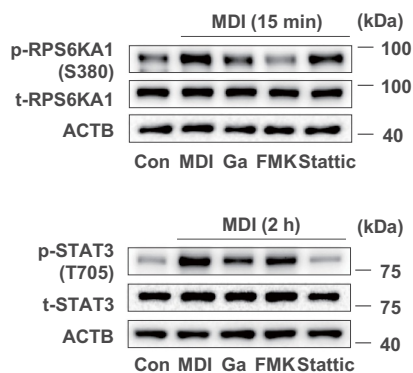
Adipogenesis is a complicated process that occurs in several stages and involves many signaling molecules [33]. To determine the influence of *G. cambogia* extract on different stages of adipogenesis during 3T3-L1 differentiation, we treated the cells with *G. cambogia* extract (300 µg/ml) for various periods of time. We found that lipid accumulation was significantly inhibited by *G. cambogia* extract at 0–2 and 2–4 days, and the inhibitory effect at 0–4 days was greater than that at 4–8 days, suggesting that the early stage of adipogenesis is potently affected by *G. cambogia* extract (Figure 1D). Consistently, we showed that CEBPA and PPARG expression was more gradually inhibited by *G. cambogia* extract at 0–4 days than at 4–8 days (Figure 1E). These results provide critical clues for the inhibitory effect of *G. cambogia* extract on early adipogenesis and related signaling molecules.

G. cambogia extract inhibits CEBPB expression

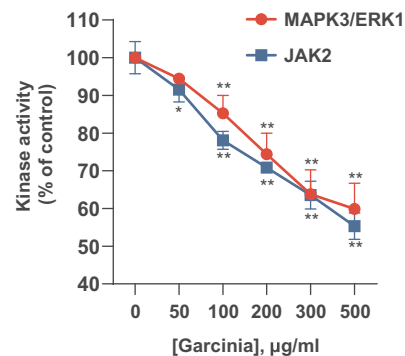
Given that *G. cambogia* extract attenuates early adipogenesis, we then examined whether *G. cambogia* extract functioned by regulating several adipogenic factors. The results of STRING analysis for construction of a protein interaction network showed that RPS6KA1 and STAT3 were highly interconnected with CEBPB and moderately interconnected with CEBPD (Fig. S2A), which act as key early regulators of adipogenesis [5,8].

To confirm the above observation, we examined the effect of *G. cambogia* extract on CEBPB and CEBPD expression.

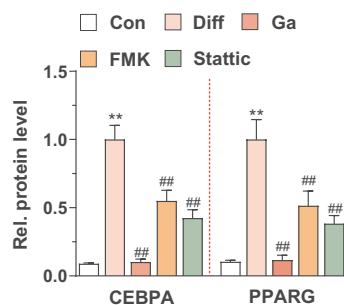
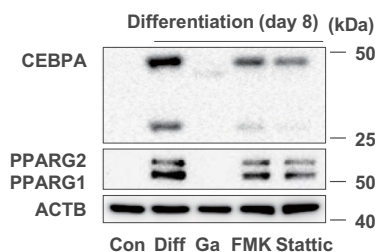
A



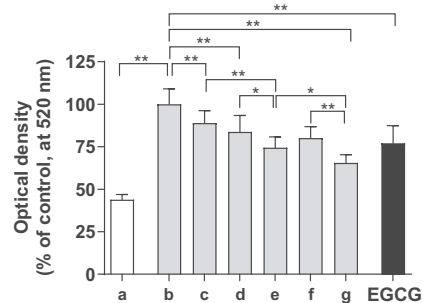
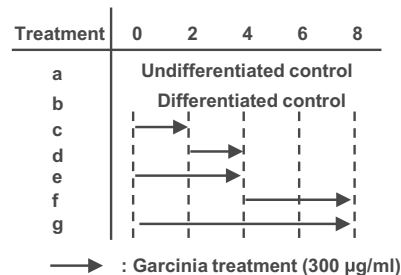
B



C



D



E

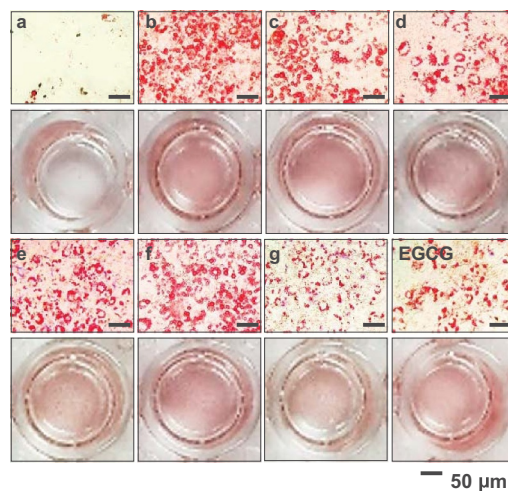
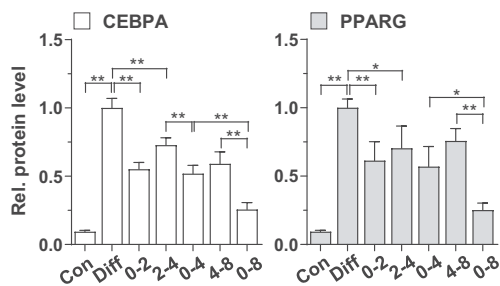
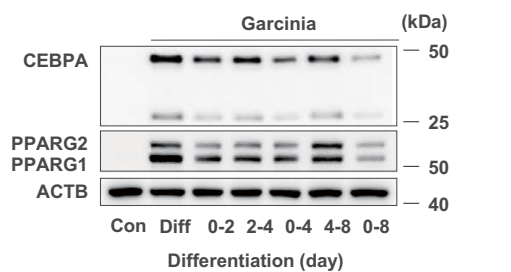


Figure 1. Antiadipogenic effect of *G. cambogia* extract and the related protein expression in 3T3-L1 preadipocytes during differentiation. (A) Effect of *G. cambogia* extract (Ga, 300 µg/ml), FMK (3 µM) and stactic (5 µM) on RPS6KA1 and STAT3 phosphorylation in MDI-induced 3T3-L1 preadipocytes (differentiation started cells) for the indicated times (n = 4 per group). Con: MDI-untreated cells, MDI: MDI-treated cells. ***p* < 0.01 vs. Con, ##*p* < 0.01 vs. MDI. (B) Kinase activity of MAPK3/ERK1 and JAK2 in response to *G. cambogia* extract (n = 4 per group). The active MAPK3/ERK1 and JAK2 enzymes were used to assess kinase activity in the presence or absence of *G. cambogia* extract at the indicated concentrations *in vitro*. **p* < 0.05 and ***p* < 0.01 vs. each control. (C) Effect of *G. cambogia* extract (300 µg/ml), FMK (3 µM) and stactic (5 µM) on CEBPA and PPARG expression in mature 3T3-L1 adipocytes (fully differentiated adipocytes) (n = 4 per group). Con: undifferentiated cells, Diff: mature 3T3-L1 adipocytes. ***p* < 0.01 vs. Con, ##*p* < 0.01 vs. Diff. (D) Effect of *G. cambogia* extract (300 µg/ml) on lipid accumulation in mature 3T3-L1 adipocytes at the indicated time points. The time table (upper) and representative images of Oil red O staining (below) are presented. EGCG (50 µM) was used as a positive control (n = 15 per group). Scale bar: 50 µm. (E) Effect of *G. cambogia* extract (300 µg/ml) on CEBPA and PPARG expression in mature 3T3-L1 adipocytes at the indicated time points (n = 4 per group). **p* < 0.05 and ***p* < 0.01 vs. each group. The data are the mean ± S.D.

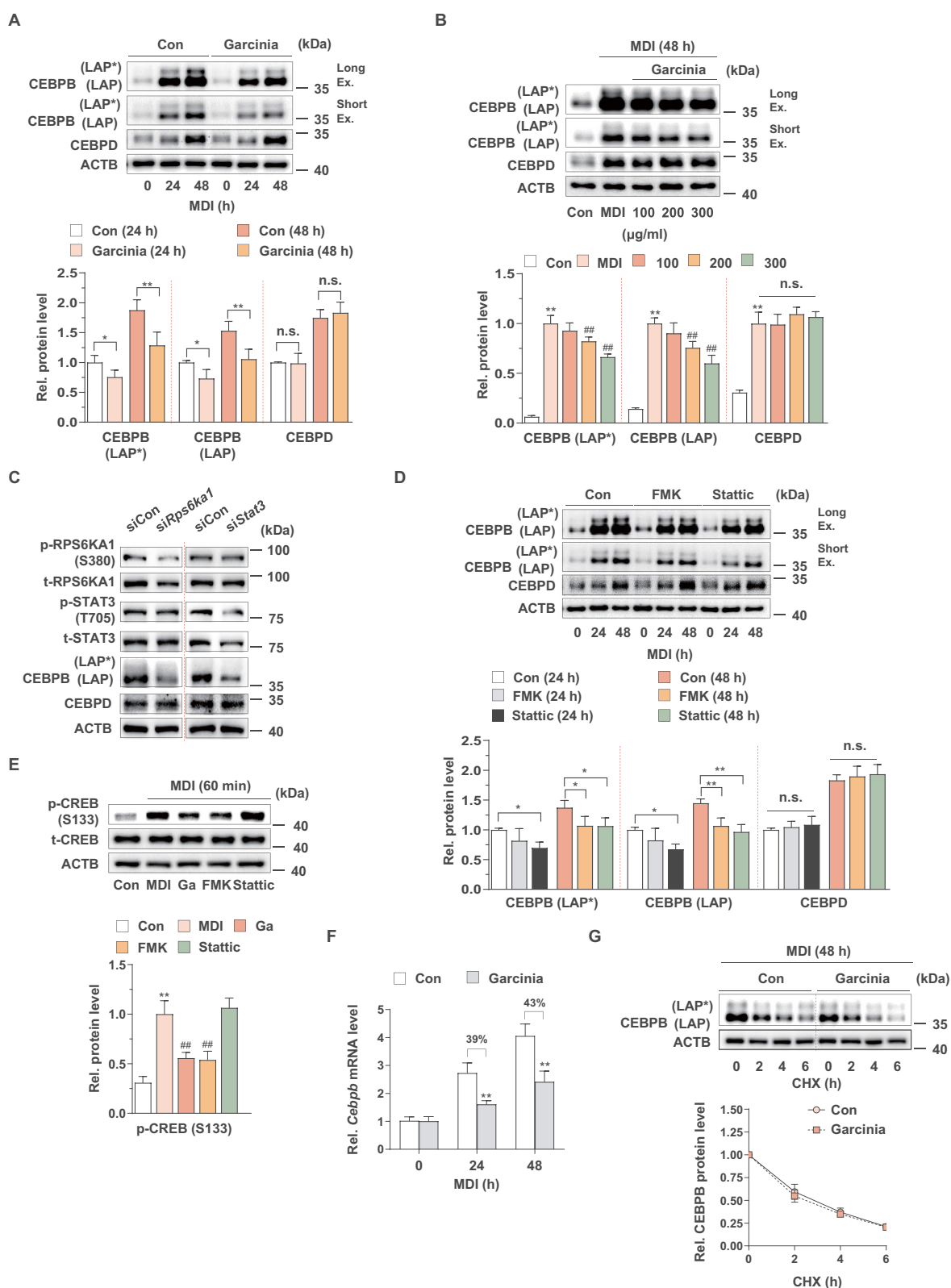


Figure 2. Effect of *G. cambogia* extract-induced RPS6KA1 and STAT3 inhibition on CEBPB regulation in MDI-induced 3T3-L1 preadipocytes during differentiation. (A) Effect of *G. cambogia* extract (300 $\mu\text{g/ml}$) on CEBPB (LAP* and LAP) and CEBPD expression in MDI-induced 3T3-L1 preadipocytes for the indicated times ($n = 4$ per group). MDI: MDI-treated cells. Ex.: Exposure. * $p < 0.05$ and ** $p < 0.01$ vs. each control. n.s.: not significant. (B) Effect of *G. cambogia* extract (0–300 $\mu\text{g/ml}$) on CEBPB (LAP* and LAP) and CEBPD expression in MDI-induced 3T3-L1 preadipocytes after 48 h ($n = 4$ per group). Con: MDI-untreated cells. ** $p < 0.01$ vs. Con, ## $p < 0.01$ vs. MDI. (C) Effect of *Rps6ka1* and *Stat3* knockdown on CEBPB (LAP* and LAP) and CEBPD expression in 3T3-L1 differentiated cells. (D) Effect of FMK (3 μM) and static (5 μM) on CEBPB (LAP* and LAP) and CEBPD expression in MDI-induced 3T3-L1 preadipocytes for the indicated duration ($n = 4$ per group). * $p < 0.05$ and ** $p < 0.01$ vs. each control. (E) Effect of *G. cambogia* extract, FMK (3 μM) and static (5 μM) on CREB phosphorylation in MDI-induced 3T3-L1 preadipocytes after 60 min ($n = 4$ per group). ** $p < 0.01$ vs. Con, ## $p < 0.01$ vs. MDI. (F) Effect of *G. cambogia* extract (300 $\mu\text{g/ml}$) on the *Cebpb* transcript level in MDI-induced 3T3-L1 preadipocytes for the indicated times ($n = 9$ per group). ** $p < 0.01$ vs. each control. (G) Effect of *G. cambogia* extract (300 $\mu\text{g/ml}$) on the CEBPB protein half-life in MDI-induced 3T3-L1 preadipocytes. After treatment of *G. cambogia* extract in cells for 42 h, translation inhibitor cycloheximide (CHX, 1.5 $\mu\text{g/ml}$) was coincubated with the indicated times ($n = 4$ per group). The data are the mean \pm S.D.

G. cambogia extract (300 µg/ml) significantly reduced MDI-induced CEBPB isoforms expression, which are full-length LAP (LAP*, liver-enriched transcriptional activating proteins) and LAP [34] without affecting CEBPD at 24 and 48 h (Figure 2A). Consistent with previous data, various concentrations of *G. cambogia* extract attenuated MDI-induced CEBPB (LAP* and LAP) expression (Figure 2B). Although we could not detect the inhibitory effect of FMK on MDI-induced RPS6KA1 phosphorylation at 24 and 48 h since MDI-induced RPS6KA1 phosphorylation peaked at 15 min and disappeared from 60 min [31], unlike STAT3 phosphorylation [35,36], we detected that stattic significantly suppressed MDI-induced STAT3 phosphorylation at 24 and 48 h (Fig. S2B). In addition, knockdown of *Rps6ka1* and *Stat3* by ~40% using small interfering RNA (siRNA) (Fig. S2C) decreased CEBPB expression without affecting CEBPD (Figure 2C). Furthermore, FMK and stattic treatment significantly inhibited MDI-induced CEBPB (LAP* and LAP) expression, indicating that RPS6KA1 and STAT3 regulate CEBPB expression (Figure 2D). To better understand the underlying molecular mechanism by which *G. cambogia* extract regulates CEBPB, we examined *Cebpb* transcription regulation and CEBPB protein stability. STAT3 regulates transcription of *Cebpb* by binding its promoter at the early stage of adipogenesis in 3T3-L1 differentiated cells [37], activated RPS6KA1 induces CREB (cAMP response element-binding protein) phosphorylation [38], and activated CREB continuously increases *Cebpb* transcription during adipogenesis [39]. *G. cambogia* extract and FMK significantly inhibited MDI-induced CREB phosphorylation, implying that *G. cambogia* extract affects *Cebpb* transcription through STAT3 and RPS6KA1-CREB (Figure 2E). As shown in Figure 2F, we found that *G. cambogia* extract significantly suppressed *Cebpb* transcript levels during MDI stimulation for 24 and 48 h. Because proteasome-mediated protein degradation is a primary means to control CEBPB expression in mammalian cells [40–42], we assessed the CEBPB half-life using a cycloheximide (CHX) chase assay. Consistent with the western blot results, *G. cambogia* extract did not affect the CEBPB half-life under MDI-induced conditions (Figure 2G). These findings, together with those shown above, reinforce the idea that *G. cambogia* extract regulates early adipogenesis by suppressing *Cebpb* transcription.

***G. cambogia* extract inhibits autophagic flux by downregulating autophagy-related gene expression**

Given that autophagy is one of the major processes involved in adipogenesis through the massive removal of intracellular components [19,43], we examined a series of proteins involved in the key steps of autophagosome formation [44]. Autophagosome formation consists of several processes, including MAP1LC3/LC3 (microtubule-associated protein 1 light chain 3) conjugation steps, which are regulated by several modules such as BECN1/beclin 1, ATG4B, ATG7, ATG3 and ATG12–ATG5 (Fig. S3A). In a time-course experiment, *G. cambogia* extract inhibited the levels of BECN1, ATG7, ATG3, LC3-I and LC3-II after 3 days of treatment (Figure 3A). However, ATG4B and ATG12–ATG5 were not affected by *G. cambogia* extract treatment (Fig. S3B). Although a decrease in LC3 levels is sometimes interpreted as evidence

of autophagy inhibition, this observation can also reflect autophagy activation through increased autolysosomal degradation [45]. Thus, SQSTM1/p62, a binding receptor of cargo proteins to autophagosomes [46], was examined, and the increased SQSTM1 levels induced by *G. cambogia* extract reflected autophagy inhibition. Consistent with the previous results, *G. cambogia* extract dose-dependently inhibited BECN1, ATG7, ATG3, LC3-I and LC3-II levels and increased SQSTM1 levels after 72 h of treatment (Figure 3B and S3C).

To verify the effect of *G. cambogia* extract on autophagic flux, we performed immunofluorescence analysis using mCherry-GFP-LC3 with LY294002 (LY) and 3-methyladenine (3-MA) (early-stage autophagy inhibitors that suppress autophagosome formation), bafilomycin A₁ (Baf, a late-stage autophagy inhibitor that blocks the fusion of autophagosomes with lysosomes) and rapamycin (Ra, autophagy activator). The yellow puncta representing GFP and RFP signals indicate immature autophagosomes, whereas autolysosomes only exhibit red fluorescence, as GFP fluorescence is lost in the acidic and proteolytic environment of the lysosome [47]. Interestingly, *G. cambogia* extract markedly decreased the number of yellow and red puncta in 3T3-L1 differentiated cells, which was similar to the effect of LY294002 and 3-MA (Figure 3C). In contrast, many yellow and few red puncta were observed in bafilomycin A₁-treated cells, and the rapamycin-treated cells exhibited the opposite effect, suggesting that *G. cambogia* extract inhibited autophagy at the early stage.

To further verify the effect of *G. cambogia* extract on autophagic flux, we analyzed the levels of LC3 and SQSTM1 compared to LY294002, 3-MA, bafilomycin A₁ and rapamycin in 3T3-L1 differentiated cells. *G. cambogia* extract decreased the levels of LC3-I and LC3-II and increased the level of SQSTM1, which was similar to the effect of LY294002 and 3-MA (Figure 3D). In contrast, bafilomycin A₁ increased the levels of LC3-I, LC3-II and SQSTM1 by blocking the degradation of LC3, and rapamycin increased the level of LC3-II and decreased levels of LC3-I and SQSTM1 through autophagy activation-mediated LC-I to LC3-II maturation. Furthermore, coincubation of *G. cambogia* extract with 3-MA and bafilomycin A₁ decreased LC-I and LC3-II expression but increased SQSTM1 expression regardless of early or late autophagy inhibition (Fig. S3D).

These results led us to hypothesize that *G. cambogia* extract regulates the transcription of autophagy-related genes since CREB and STAT3, which are affected by *G. cambogia* extract, act as transcription factors to regulate autophagy-related genes [48,49]. Thus, we measured the transcript levels of *Becn1*, *Atg7*, *Atg3*, *Lc3* and *Sqstm1* in the time-course experiments and observed that *G. cambogia* extract significantly inhibited *Becn1*, *Atg7*, *Atg3* and *Lc3* levels and increased *Sqstm1* level (Figure 3E). In addition, the degree of transcript level alteration was maintained or increased during differentiation periods except for *Sqstm1* at day 6, suggesting that the inhibitory effect of *G. cambogia* extract on autophagic flux and protein expression was attributed, at least in part, to the regulation of transcription.

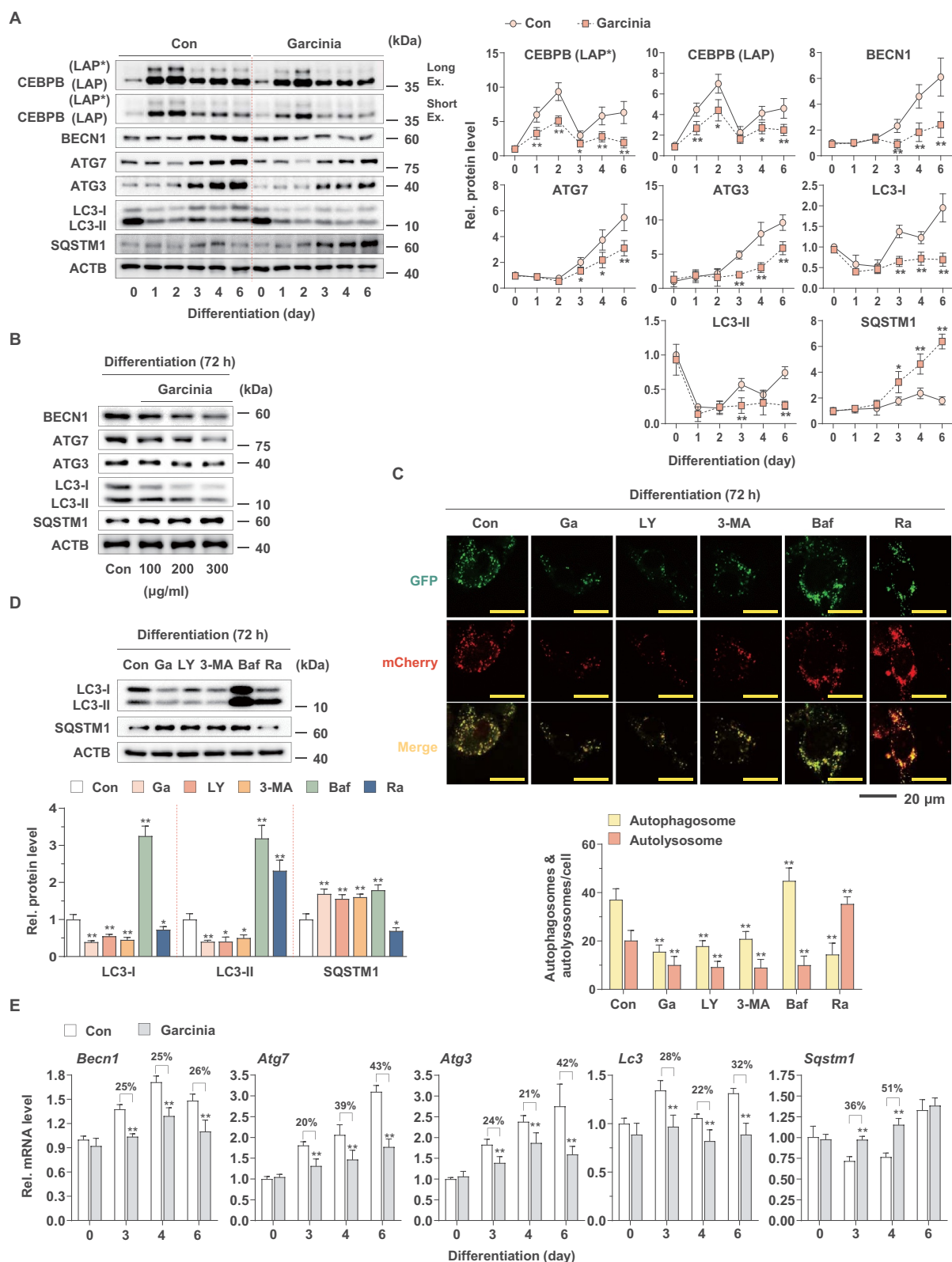
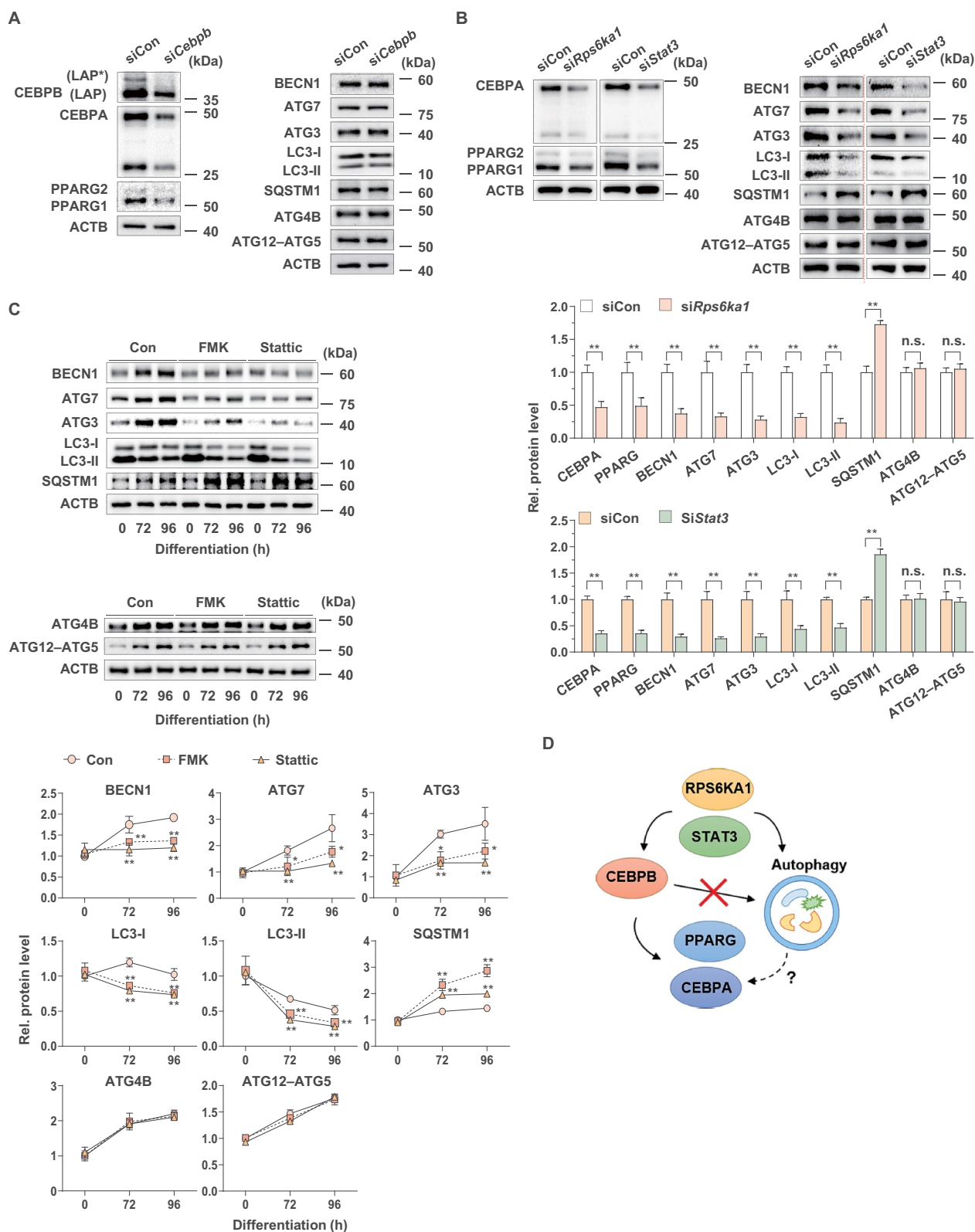


Figure 3. Effect of *G. cambogia* extract on autophagic flux and autophagy-related gene expression in 3T3-L1 preadipocytes during differentiation. (A) Effect of *G. cambogia* extract (300 µg/ml) on CEBPB (LAP* and LAP), BECN1, ATG7, ATG3, LC3 and SQSTM1 expression in 3T3-L1 differentiated cells for the indicated times ($n = 4$ per group). * $p < 0.05$ and ** $p < 0.01$ vs. each control. (B) Effect of *G. cambogia* extract (0–300 µg/ml) on BECN1, ATG7, ATG3, LC3 and SQSTM1 expression in 3T3-L1 differentiated cells for 72 h ($n = 4$ per group). (C) Fluorescence photographs and quantification data of mCherry-GFP-LC3 puncta in 3T3-L1 differentiated cells in response to *G. cambogia* extract (Ga, 300 µg/ml) for 72 h, LY294002 (LY, 10 µM), 3-methyladenine (3-MA, 0.5 mM), bafilomycin A₁ (Baf, 100 µM) and rapamycin (Ra, 10 nM) for 24 h. The average number of autophagosomes (yellow) and autolysosomes (red) per cell was determined and analyzed ($n = 9$ per group). Scale bar: 20 µm. ** $p < 0.01$ vs. each control. (D) Effect of *G. cambogia* extract (Ga, 300 µg/ml, 72 h), LY294002 (LY, 10 µM, 24 h), 3-methyladenine (3-MA, 0.5 mM, 24 h), bafilomycin A₁ (Baf, 100 µM, 24 h) and rapamycin (Ra, 10 nM, 24 h) on LC3 and SQSTM1 expression in 3T3-L1 differentiated cells ($n = 4$ per group). * $p < 0.05$ and ** $p < 0.01$ vs. each control. (E) Effect of *G. cambogia* extract (300 µg/ml) on the transcript levels of *Becn1*, *Atg7*, *Atg3*, *Lc3* and *Sqstm1* in 3T3-L1 differentiated cells for the indicated times ($n = 9$ per group). ** $p < 0.01$ vs. each control. The data are the mean \pm S.D.



Suppression of RPS6KA1 and STAT3 by *G. cambogia* extract mediates autophagy regulation

It has been previously reported that CEBPB is required for the activation of autophagy during 3T3-L1 adipocyte differentiation [50]. Thus, we hypothesized that CEBPB downregulation by *G. cambogia* extract contributed to autophagic flux regulation. With *Cebpb* siRNA, the *Cebpb* transcript was knocked down by ~ 50% compared to that of the control siRNA (Fig. S4). Knockdown of *Cebpb* inhibited CEBPB, CEBPA and PPARG expression compared to the control group, while autophagy-related proteins, such as BECN1, ATG7, ATG3, LC3-I and LC3-II, SQSTM1, ATG4B and ATG12-ATG5, were not changed, which was in conflict with a previous report [50] (Figure 4A).

To determine whether RPS6KA1 and STAT3 regulate autophagy activation, we blocked *Rps6ka1* and *Stat3* expression using siRNA, and *Rps6ka1* and *Stat3* knockdown altered the levels of BECN1, ATG7, ATG3, LC3-I and LC3-II, SQSTM1, CEBPA and PPARG without affecting ATG4B and ATG12-ATG5 (Figure 4B). In addition, we treated 3T3-L1 differentiated cells with FMK and stattic to inhibit RPS6KA1 and STAT3 phosphorylation. FMK and stattic reduced BECN1, ATG7, ATG3, LC3-I and LC3-II levels and increased SQSTM1 levels (Figure 4C). In addition, ATG4B and ATG12-ATG5 expression was unchanged by FMK and stattic. These data indicate that *G. cambogia* extract-mediated inhibition of RPS6KA1 and STAT3, but not CEBPB, is essential for autophagy regulation in adipocytes (Figure 4D).

G. cambogia extract increases KLF3 level by RPS6KA1- and STAT3-mediated autophagy regulation

Adipogenesis is regulated by the interactions of a series of positive and negative regulators [33]. Since autophagy promotes adipocyte differentiation by controlling the degradation of negative regulators [19], we hypothesized that *G. cambogia* extract-mediated autophagy inhibition affected adipocyte differentiation by controlling the degradation of negative regulators. Among several regulators, KLF2 and KLF3 have been reported to repress the transactivation of *Pparg* and *Cebpa* [11]. We found that *G. cambogia* extract (300 µg/ml) increased KLF3 level and decreased CEBPA and PPARG levels compared to those of the control from day 3 after starting differentiation (Figure 5A). Consistent with the time-course results, *G. cambogia* extract dose-dependently enhanced KLF3 level and inhibited CEBPB, CEBPA and PPARG levels at 72 h of treatment (Figure 5B). However, KLF2 was not affected by *G. cambogia* extract treatment (Fig. S5A and B), suggesting that the observed effects were KLF2-independent.

To further verify whether RPS6KA1, STAT3 and CEBPB could regulate KLF3 expression, we analyzed KLF3 level in FMK-, stattic- and siRNA-treated cells. Suppression of RPS6KA1 and STAT3 by specific inhibitors significantly increased KLF3 level and decreased CEBPB, CEBPA and PPARG levels (Figure 5C). In addition, *Rps6ka1* and *Stat3*

knockdown increased KLF3 level, but *Cebpb* knockdown did not affect KLF3 level indicating that regulation of KLF3 is via RPS6KA1 and STAT3, not CEBPB (Figure 5D).

Since several autophagy-related genes were regulated by *G. cambogia* extract, we evaluated the *Klf3* transcript level, which was found to be unaffected by *G. cambogia* extract, suggesting other regulatory possibilities (Figure 5E). To determine whether *G. cambogia* extract affects KLF3 protein degradation, cells were treated with CHX alone or in combination with *G. cambogia* extract for the indicated time. We observed that KLF3 half-life was significantly increased by *G. cambogia* extract plus CHX compared to CHX alone, indicating that *G. cambogia* extract significantly decreased the protein degradation rate of KLF3 (Figure 5F). Since autophagy and ubiquitin-proteasome system (UPS) are major protein degradation pathways in eukaryotic cells [51,52], we examined whether autophagy or proteasome contributes to the degradation of KLF3 using 3-MA (autophagy inhibitor) and MG132 (proteasome inhibitor). Like *G. cambogia* extract, 3-MA significantly increased the expression of SQSTM1 and KLF3, however, MG132 did not, suggesting that autophagy plays a main role in degrading KLF3 and SQSTM1 proteins during adipogenesis (Figure 5G). In addition, inhibition of autophagic flux using LY294002, 3-MA and bafilomycin A₁ increased KLF3 level and decreased CEBPA and PPARG levels, similar to the effect of *G. cambogia* extract, but rapamycin, an autophagy activator, reduced KLF3 level, and enhanced CEBPA and PPARG levels suggesting that autophagy regulates KLF3 in 3T3-L1 differentiated cells (Fig. S5C). Similar to the alteration of protein expression, LY294002, 3-MA and bafilomycin A₁ alone had inhibitory effects on lipid accumulation and additively suppressed *G. cambogia* extract-mediated lipid accumulation inhibition (Fig. S5D). Although rapamycin alone did not affect lipid accumulation, the inhibitory effect of *G. cambogia* extract on lipid accumulation was attenuated by cotreatment, implying an autophagy-activating effect.

G. cambogia extract inhibits SQSTM1-mediated selective autophagy degradation of KLF3

SQSTM1 is important for selective autophagy action because the cargo proteins bind to SQSTM1 receptor protein and are sequestered to autophagy-specific modifiers, such as LC3 [53]. Thus, we examined whether the increased SQSTM1 by *G. cambogia* extract, FMK and stattic interacted with KLF3. As shown in Figure 6A, the level of SQSTM1 that physically interacted with KLF3 was increased by *G. cambogia* extract, FMK and stattic, but the ratio of SQSTM1 versus KLF3 was not significantly changed, implying that *G. cambogia* extract-mediated inhibition of RPS6KA1 and STAT3 did not affect the ability of SQSTM1 to interact with KLF3 as a cargo protein. To verify the role of SQSTM1 in the regulation of KLF3 in *G. cambogia* extract-treated cells, *Sqstm1* siRNA was treated to knockdown *Sqstm1*

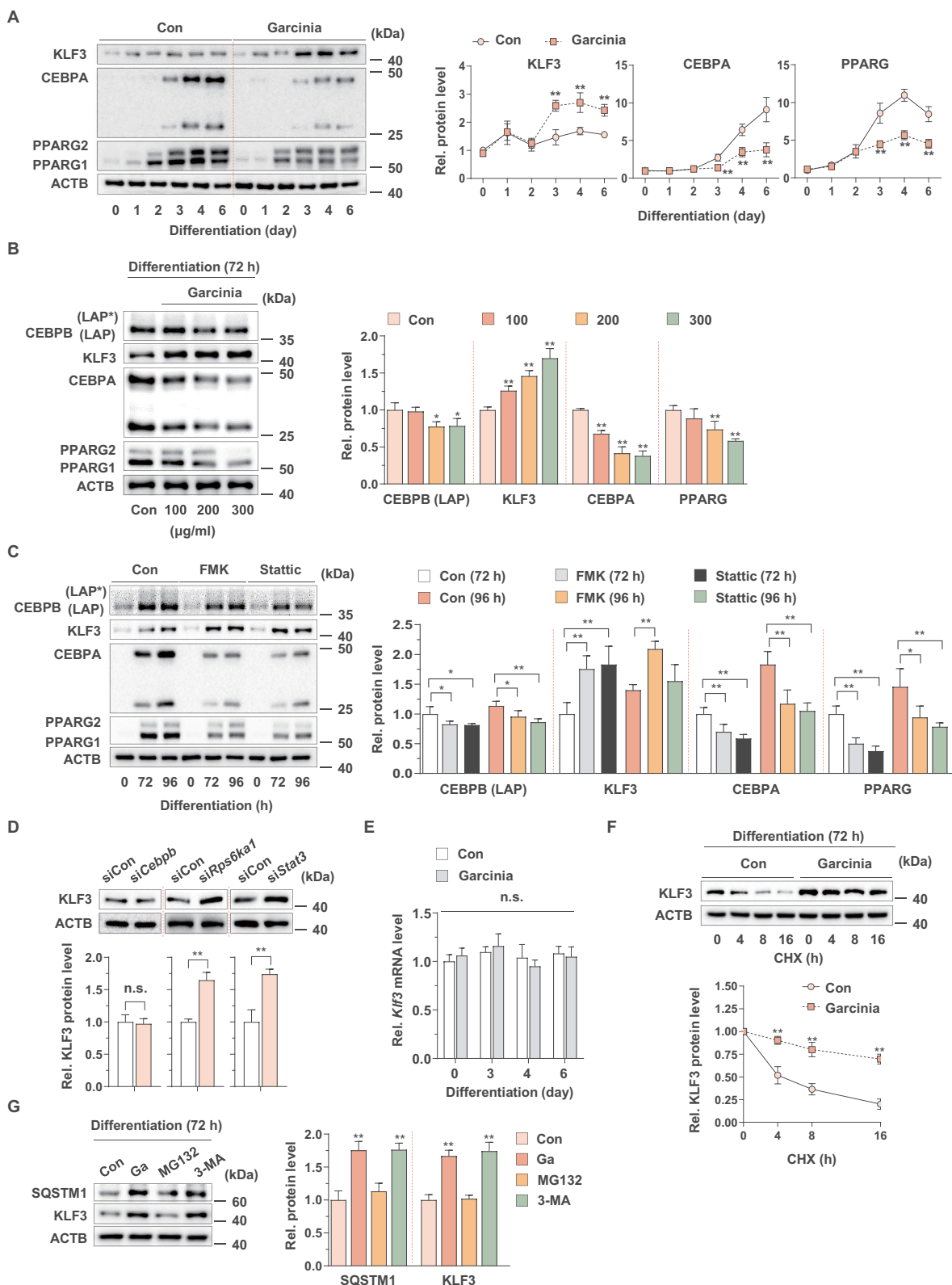


Figure 5. Effect of *G. cambogia* extract on KLF3 expression in 3T3-L1 preadipocytes during differentiation. (A) Effect of *G. cambogia* extract (300 µg/ml) on KLF3, CEBPA and PPARG in 3T3-L1 differentiated cells for the indicated times ($n = 4$ per group). $**p < 0.01$ vs. each control. (B) Effect of *G. cambogia* extract (0–300 µg/ml) on CEBPB, KLF3, CEBPA and PPARG expression in 3T3-L1 differentiated cells after 72 h ($n = 4$ per group). $*p < 0.05$ and $**p < 0.01$ vs. Con. (C) Effect of FMK (3 µM) and stattic (5 µM) on CEBPB, KLF3, CEBPA and PPARG expression in 3T3-L1 differentiated cells for the indicated times ($n = 4$ per group). $*p < 0.05$ and $**p < 0.01$ vs. each control. (D) Effect of *Cebpb*, *Rps6ka1* and *Stat3* knockdown on KLF3 expression in 3T3-L1 differentiated cells after 72 h ($n = 4$ per group). $**p < 0.01$ vs. siCon. n.s.: not significant. (E) Effect of *G. cambogia* extract (300 µg/ml) on *Klf3* transcript levels in 3T3-L1 differentiated cells for the indicated times ($n = 9$ per group). (F) Effect of *G. cambogia* extract (300 µg/ml) on the KLF3 protein half-life in 3T3-L1 differentiated cells after 72 h. After treatment of *G. cambogia* extract in cells, cycloheximide (CHX, 1.5 µg/ml) was coincubated with the indicated times ($n = 4$ per group). $**p < 0.01$ vs. each control. (G) Effect of *G. cambogia* extract (Ga, 300 µg/ml) for 72 h and MG132 (10 µM) and 3-MA (0.5 mM) for 24 h on SQSTM1 and KLF3 expression in 3T3-L1 differentiated cells ($n = 4$ per group). $**p < 0.01$ vs. Con. The data are the mean \pm S.D.

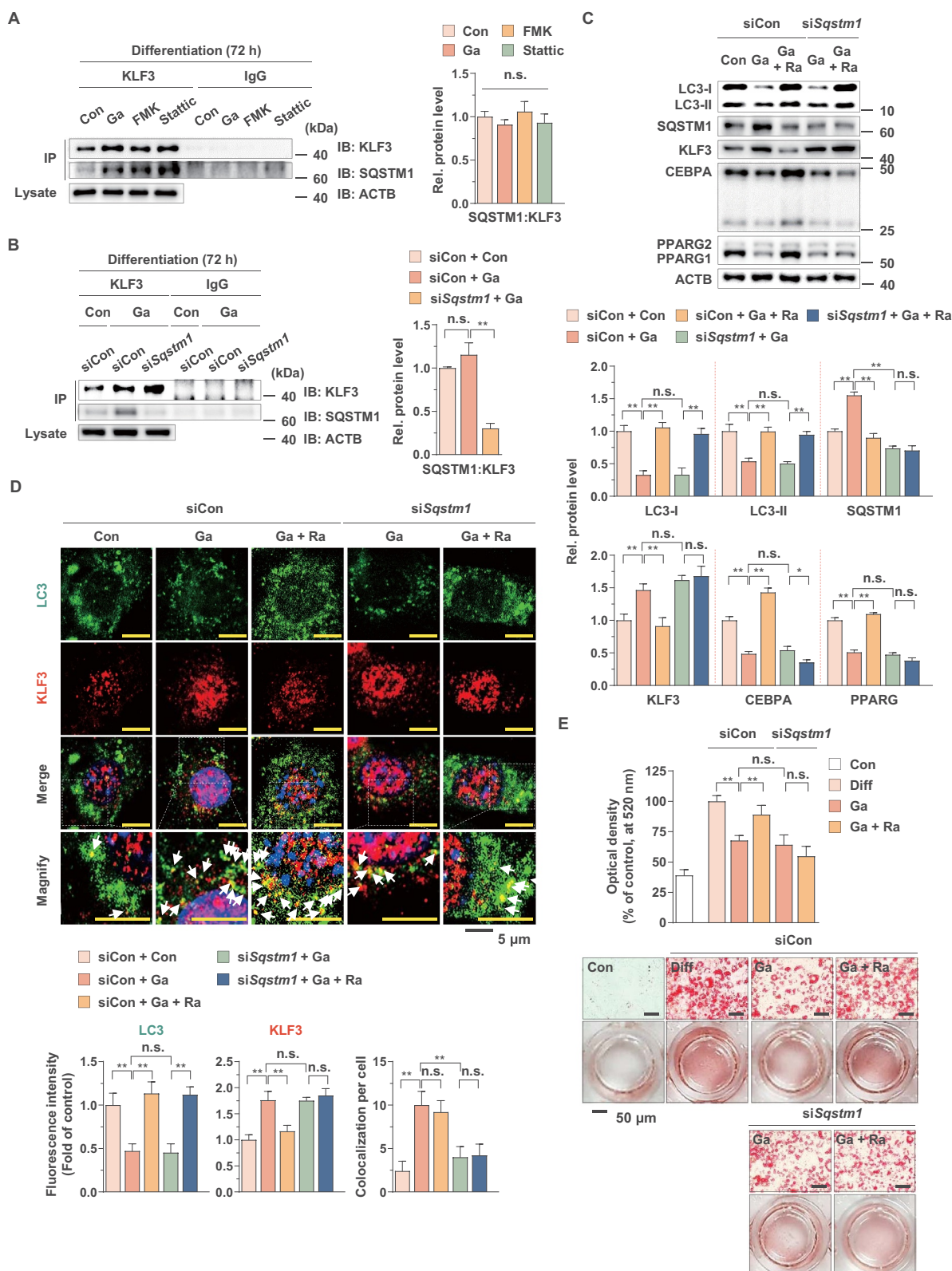


Figure 6. Effect of *G. cambogia* extract on SQSTM1-mediated selective autophagic degradation of KLF3 in 3T3-L1 preadipocytes during differentiation. (A) Interaction of SQSTM1 and KLF3 in 3T3-L1 differentiated cells treated with *G. cambogia* extract (Ga, 300 μ g/ml), FMK (3 μ M) and stattic (5 μ M) for 72 h. Coimmunoprecipitation (IP) was used to analyze the level of SQSTM1 that physically interacted with KLF3. The lysates were immunoprecipitated with anti-KLF3 and anti-IgG antibodies, and the precipitates were analyzed by western blotting using antibodies against SQSTM1 and KLF3 ($n = 4$ per group). (B) Effect of *Sqstm1* knockdown on the interaction of SQSTM1 and KLF3 in 3T3-L1 differentiated cells treated with *G. cambogia* extract (300 μ g/ml). *Sqstm1* knockdown cells were treated with *G. cambogia* extract (300 μ g/ml) for 72 h ($n = 4$ per group). (C) Effect of *Sqstm1* knockdown on LC3, SQSTM1, KLF3, CEBPA and PPARG expression in 3T3-L1 differentiated cells treated with *G. cambogia* extract (300 μ g/ml) for 72 h in the presence or absence of rapamycin (Ra, 10 nM) for 24 h ($n = 4$ per group). (D) Fluorescence photographs (left) and quantification data (below) of LC3 and KLF3 in *Sqstm1* knockdown cells treated with *G. cambogia* extract (300 μ g/ml) for 72 h in the presence or absence of rapamycin (10 nM) for 24 h. The fluorescence intensity of FITC (i.e., LC3) and TRITC (i.e., KLF3) was quantified using ImageJ software and colocalization (yellow dots indicated by white arrows) of FITC and TRITC per cell was determined and analyzed ($n = 5$ per group). Scale bars: 5 μ m (E) Effect of *Sqstm1* knockdown on *G. cambogia* extract- and rapamycin-mediated lipid accumulation in mature 3T3-L1 adipocytes ($n = 12$ per group). During full differentiation (day 0–8), cells were treated with *G. cambogia* extract (300 μ g/ml), and rapamycin (10 nM) was added at day 3–8. Con: undifferentiated cells, Diff: mature 3T3-L1 adipocytes. * $p < 0.05$ and ** $p < 0.01$ vs. each group. n.s.: not significant. The data are the mean \pm S.D.

transcript by ~ 80% as compared to that of the control siRNA (Fig. S6) and reduced the ratio of SQSTM1 versus KLF3 in *G. cambogia* extract-treated cells (Figure 6B). The ability of *G. cambogia* extract to inhibit autophagy flux (decreased LC3-I and LC3-II expression and increased SQSTM1) and adipogenic factors (CEBPA and PPARG), and increase KLF3 level was reversed by cotreatment of rapamycin (Figure 6C). However, the effect of rapamycin on KLF3 inhibition was abolished by *Sqstm1* knockdown. In addition, *Sqstm1* knockdown impaired the sequestration of KLF3 to LC3 puncta (autophagosome marker) as shown in yellow dots and did not induce the reduction of KLF3 level (shown in red) in cotreatment of *G. cambogia* extract and rapamycin, indicating that SQSTM1 plays an important role in selective autophagic degradation of KLF3 (Figure 6D). Furthermore, rapamycin-induced increased lipid accumulation was blocked by *Sqstm1* knockdown in *G. cambogia* extract-treated cells (Figure 6E). Taken together, these results suggest that *G. cambogia* extract inhibited SQSTM1-mediated selective autophagic degradation of KLF3 by suppressing autophagic flux, resulting in the interaction of SQSTM1 to KLF3 to remain, and adipogenesis would be inhibited by reducing the expression of CEBPA and PPARG.

Increased KLF3-CTBP2 interaction by *G. cambogia* extract-mediated RPS6KA1 and STAT3 inhibition attenuates *Cebpa* and *Pparg* transcription

KLF3 functions as a transcriptional repressor of target gene via recruitment of transcriptional corepressor such as CTBP [11,16]. Thus, we examined effect of *G. cambogia* extract, FMK and stattic on CTBP1 and 2 expression and found that these did not affect CTBPs expression (Figure 7A,B, S7A and B). However, the physical interaction level of CTBP2, but not CTBP1, with KLF3 was increased, but the ratio of CTBP2 versus KLF3 was not changed by *G. cambogia* extract, FMK and stattic, which indicated that increased KLF3 by RPS6KA1 and STAT3 inhibition formed the transcriptional complex with CTBP2 (Figure 7C and S7C). In accordance with previous results, CTBP2 intensity was not affected by *G. cambogia* extract, FMK and stattic, but the colocalization of CTBP2 and KLF3 in nucleus was increased by *G. cambogia* extract, FMK and stattic using confocal microscopic analysis (Figure 7D). Furthermore, *G. cambogia* extract significantly inhibited the transcription of *Cebpa* and *Pparg*, which are target genes of KLF3-CTBP2, as well as CEBPB to induce adipogenesis. (Figure 7E). Thus, our results suggest that increased KLF3 induced by *G. cambogia* extract, FMK and stattic can form a transcriptional repressor complex with CTBP2 and affect, at least in part, the inhibition of *Cebpa* and *Pparg* transcription.

***G. cambogia* extract suppresses increases in body weight and adipose tissue mass in HFD-induced obese mice**

To investigate the physiological effect of *G. cambogia* extract on adipose tissue in obesity, mice were fed a normal diet (ND), high-fat diet (HFD) or HFD plus *G. cambogia* extract

starting at 5 weeks of age. After 8 weeks, the body weights of HFD-fed mice were significantly increased compared to those of ND-fed mice, and low-dose (200 mg/kg) and high-dose (400 mg/kg) *G. cambogia* extract and orlistat (20 mg/kg, antiobesity drug as a positive control) reduced body weight gain without significant differences in food intake and caloric intake (Figure 8A,B and S8A and B). The HFD-fed mice showed a higher energy efficiency ratio (EER) than ND-fed mice, and the increased EER was decreased by *G. cambogia* extract and orlistat administration. At the end of the experiment, various regions of adipose tissues and organs were collected, weighed and examined for pathological changes. The gross sizes of epididymal (eWAT), retroperitoneal (rWAT), and inguinal subcutaneous (iWAT) white adipose tissue from *G. cambogia* extract-administered mice were markedly smaller than those of HFD-fed mice (Figure 8C-E). For further analysis, we selected eWAT and iWAT because these regions of fat mass significantly decreased and examined the effect of *G. cambogia* extract on adipocyte size since hypertrophy is a critical process of adipogenesis [54]. The administration of *G. cambogia* extract significantly increased the number of small adipocytes in both eWAT and iWAT (Figure 8F), and there was no sign of obvious pathological changes in major organs, such as the heart, spleen, lung and kidney, in the high-dose (400 mg/kg) *G. cambogia* extract-administered mice, indicating that *G. cambogia* extract exhibited an inhibitory effect on adipocyte size without other organ toxicity (Fig. S8C). In addition, *G. cambogia* extract attenuated HFD-induced hepatic lipid deposition and improved glucose homeostasis, similar to previous reports (Fig. S8D and E) [55–57]. Furthermore, *G. cambogia* extract ameliorated HFD-induced abnormal serum chemistry levels. The increased triglyceride, total cholesterol, GPT/ALT (glutamic pyruvic transaminase, soluble) and GOT1/AST (glutamic-oxaloacetic transaminase 1, soluble) levels were abrogated by *G. cambogia* extract (Figure 8G and S8F). Taken together, *G. cambogia* extract attenuated HFD-induced body weight gain, adipose tissue accumulation and adipocyte size enlargement and improved the regulation of abnormal serum chemistry levels and metabolic phenotype, which were likely associated with decreased energy efficiency.

Analysis of *G. cambogia* extract-mediated regulation of the identified targets in obese animal models

To clarify the regulation of identified targets by *G. cambogia* extract in adipose tissue, we performed western blotting of eWAT and iWAT from mice fed a ND, HFD, and HFD plus a high dose of *G. cambogia* (400 mg/kg). We found that HFD feeding induced RPS6KA1 and STAT3 phosphorylation, LC3-I and LC3-II activation, SQSTM1 and KLF3 inhibition, and CEBPA and PPARG activation (Figure 9A and B). These signaling alterations were alleviated by *G. cambogia* extract. In addition, the identified targets, RPS6KA1 and STAT3 phosphorylation, and LC3-I and LC3-II expression showed strong positive correlations (Fig. S9A and B). In contrast, RPS6KA1 and STAT3 phosphorylation and SQSTM1 and KLF3 expression showed strong negative correlations, which supported that RPS6KA1 and STAT3 activation induced

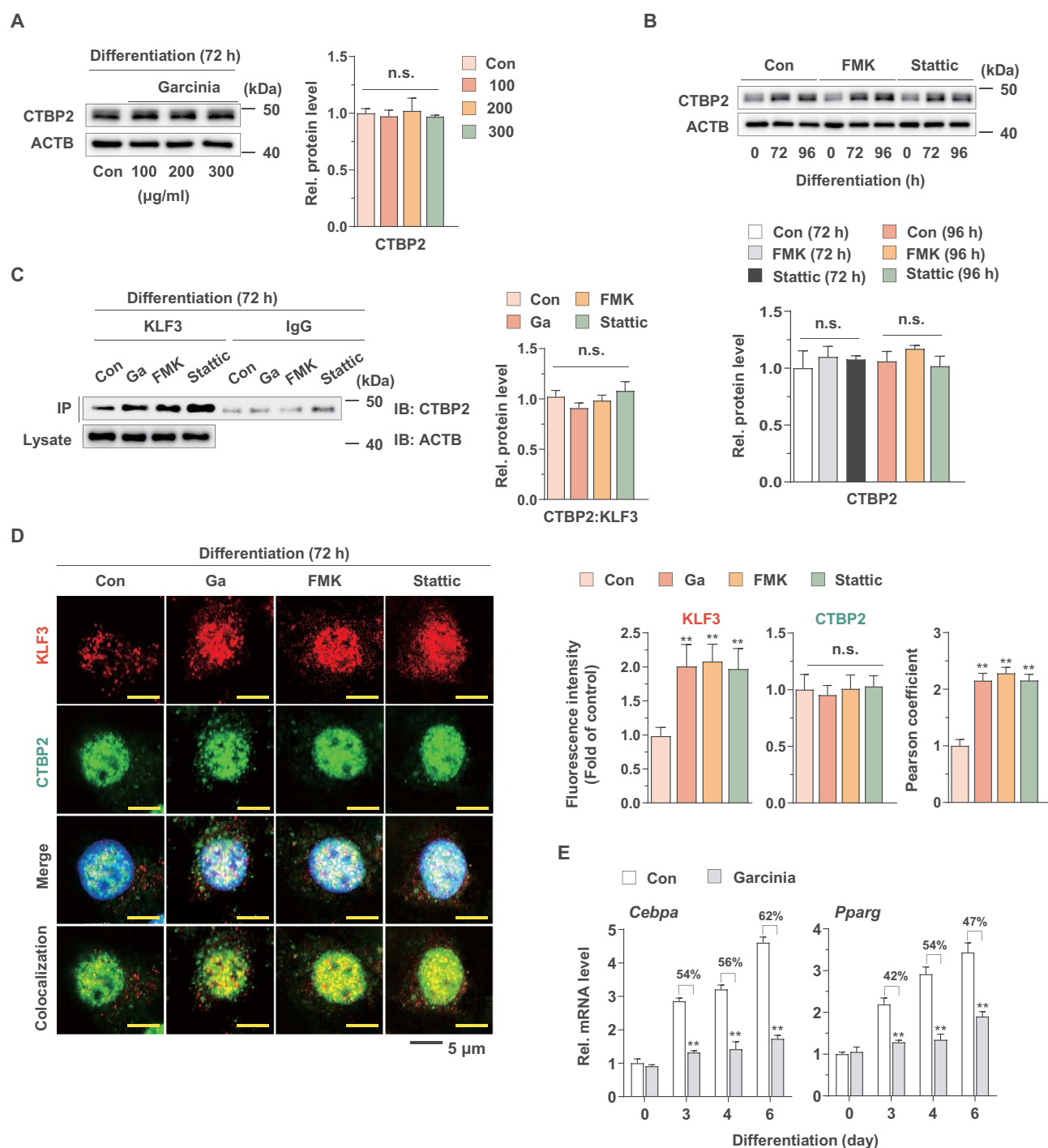


Figure 7. Effect of *G. cambogia* extract on KLF3 and CTBP2 interaction to regulate adipogenic factors in 3T3-L1 preadipocytes during differentiation. (A) Effect of *G. cambogia* extract (0–300 µg/ml) on CTBP2 expression in 3T3-L1 differentiated cells for 72 h ($n = 4$ per group). n.s.: not significant. (B) Effect of FMK (3 µM) and static (5 µM) on CTBP2 expression in 3T3-L1 differentiated cells for the indicated times ($n = 4$ per group). (C) Physical interaction of KLF3 and CTBP2 in 3T3-L1 differentiated cells treated with *G. cambogia* extract (Ga, 300 µg/ml), FMK (3 µM) and static (5 µM) for 72 h. Coimmunoprecipitation (IP) was used to analyze the interaction of KLF3 and CTBP2. The lysates were immunoprecipitated with anti-KLF3 and anti-IgG antibodies, and the precipitates were analyzed by western blotting using antibody against CTBP2 ($n = 4$ per group). (D) Fluorescence photographs (left) and quantification data (right) of KLF3 and CTBP2 in 3T3-L1 differentiated cells treated with *G. cambogia* extract (300 µg/ml), FMK (3 µM) and static (5 µM) for 72 h. The fluorescence intensity and colocalization of TRITC (i.e., KLF3) and FITC (i.e., CTBP2) were quantified using ImageJ software. Colocalization was analyzed using the Pearson correlation coefficient. Scale bars: 5 µm. ($n = 6$ per group). $^{***}p < 0.01$ vs. Con, n.s.: not significant. (E) Effect of *G. cambogia* extract (300 µg/ml) on the transcript levels of *Cebpa* and *Pparg* in 3T3-L1 differentiated cells for the indicated times ($n = 9$ per group). $^{***}p < 0.01$ vs. each control. The data are the mean \pm S.D.

autophagy in adipose tissues, contributing to KLF3 degradation (Fig. S9C and 9 C). Moreover, the expression and nuclear translocation of phospho-RPS6KA1, phospho-STAT3 and KLF3 were detected by inverse patterns in eWAT and iWAT (Figure 9D,E and S9D).

To verify the association between KLF3 and autophagy, we analyzed the correlations between KLF3 and LC3 and SQSTM1 proteins in eWAT and iWAT. Significant negative correlations between KLF3 and LC3-I and LC3-II proteins and positive correlations between KLF3 and SQSTM1

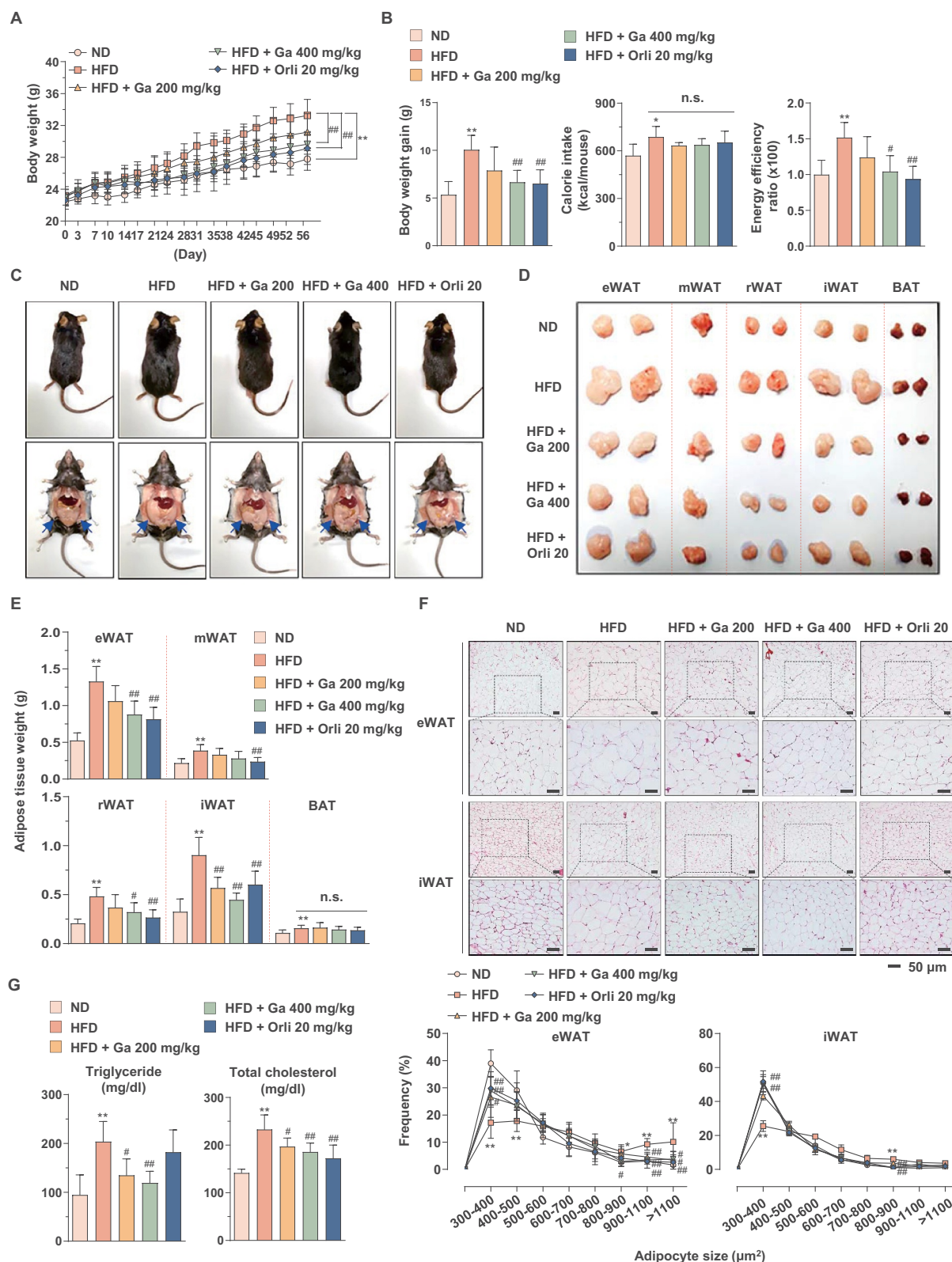


Figure 8. Effect of *G. cambogia* extract on HFD-induced obesity in mice. (A) Effect of *G. cambogia* extract on high-fat diet (HFD)-induced body weight, and (B) weight gain, caloric intake and energy efficiency rate (EER) ($n = 8$ per group). Body weight and food intake were monitored twice per week for 8 weeks. Normal diet (ND)-fed mice served as a negative control for high-fat accumulation, and orlistat (20 mg/kg) was used as a positive control for antiobesity effects. (C and D) Effect of *G. cambogia* extract on HFD-induced adipose fat tissue mass and (E) quantification data ($n = 8$ per group). eWAT: epididymal white adipose tissue; mWAT: mesenteric white adipose tissue; rWAT: retroperitoneal white adipose tissue; iWAT: inguinal subcutaneous white adipose tissue; BAT: brown adipose tissue. (F) Effect of *G. cambogia* extract on adipocyte size in HFD-induced eWAT and iWAT. H&E staining of eWAT and iWAT was performed for histological analysis, and adipocyte size was estimated using ImageJ software Adiposoft. Scale bars: 50 μm . (G) Serum analysis of triglyceride and total cholesterol levels ($n = 7$ per group). * $p < 0.05$, ** $p < 0.01$ vs. ND-fed mice, # $p < 0.05$ and ## $p < 0.01$ vs. HFD-fed mice. n.s.: not significant. The data are the mean \pm S.D.

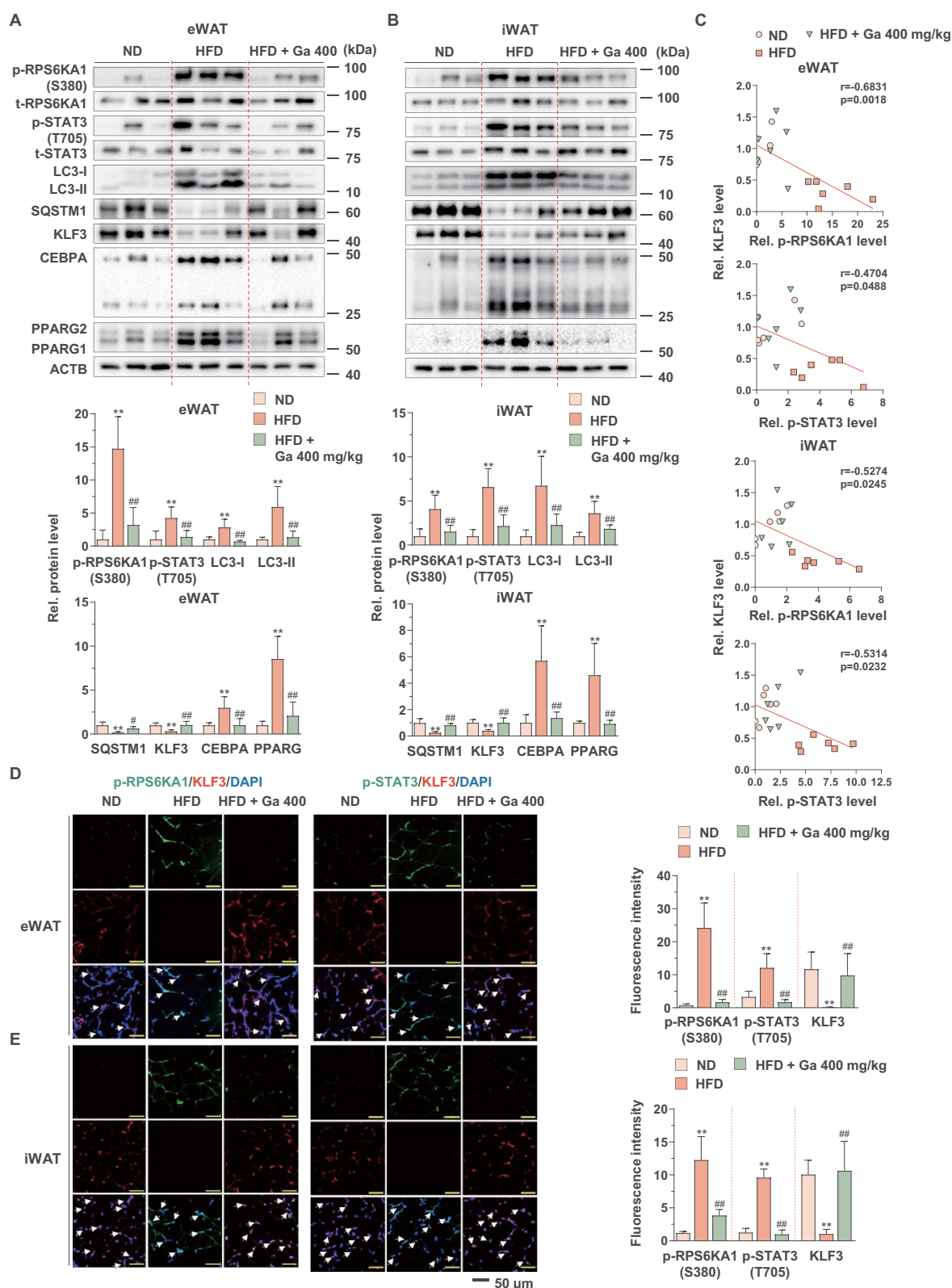


Figure 9. Effect of *G. cambogia* extract on the identified targets in HFD-induced adipose tissues. (A and B) Effect of *G. cambogia* extract on phospho- and total-RPS6KA1, phospho- and total-STAT3, LC3, SQSTM1, KLF3, CEBPA and PPARG expression of eWAT and iWAT in ND-fed, HFD-fed and HFD-fed mice administered a high dose of *G. cambogia* extract (400 mg/kg) ($n = 6$ per group). (C) Correlations between phospho-RPS6KA1, phospho-STAT3 and KLF3 protein expression in eWAT and iWAT ($n = 6$ per group). Each point represents one sample. (D and E) Immunofluorescence analysis of phospho-RPS6KA1, phospho-STAT3 and KLF3 expression in eWAT and iWAT ($n = 4$ per group). Nuclei were stained with DAPI (blue), and white arrows indicate phospho-RPS6KA1, phospho-STAT3 and KLF3 colocalization with DAPI. Scale bars, 50 μ m. ****** $p < 0.01$ vs. ND-fed mice, **#** $p < 0.05$ and **###** $p < 0.01$ vs. HFD-fed mice. The data are the mean \pm S.D.

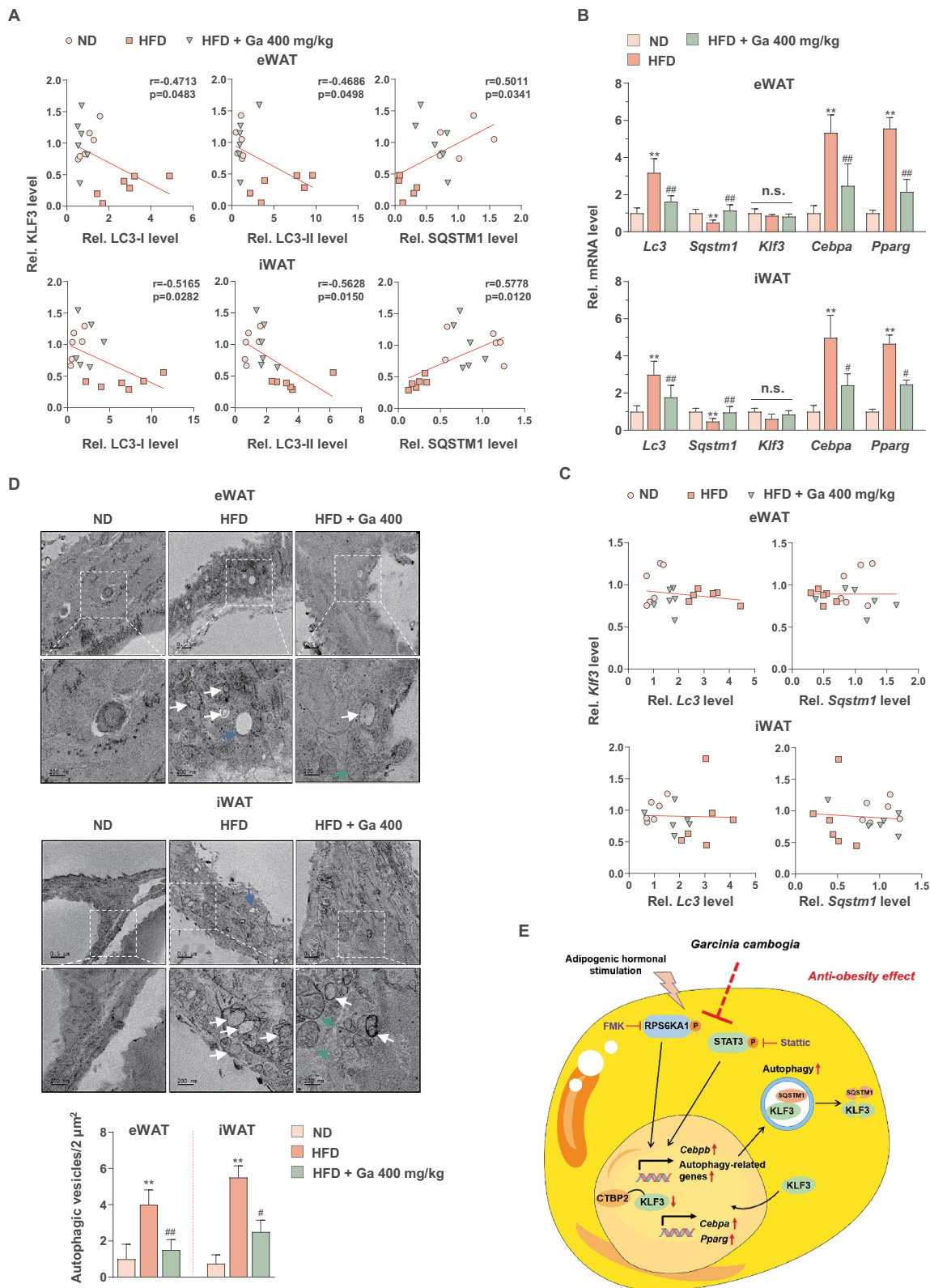


Figure 10. Analysis of the adipose tissues in the animal model. (A) Correlations between LC3-I, LC3-II, SQSTM1 and KLF3 protein expression in eWAT and iWAT ($n = 6$ per group). Each point represents one sample. (B) *Lc3*, *Sqstm1*, *Klf3*, *Cebpa* and *Pparg* transcript levels of eWAT and iWAT in ND-fed, HFD-fed and HFD-fed mice administered a high dose of *G. cambogia* extract (400 mg/kg) ($n = 6$ per group). (C) Correlations between *Klf3*, *Lc3* and *Sqstm1* transcript levels in eWAT and iWAT ($n = 6$ per group). Each point represents one sample. (D) Representative transmission electron micrographs of eWAT and iWAT in ND-fed, HFD-fed and HFD-fed mice administered a high dose of *G. cambogia* extract (400 mg/kg). The lower images are the enlarged representations of the boxed regions of the upper images. Scale bars: upper, 0.5 μm ; lower, 200 nm. Autophagic vesicles are highlighted by white arrows and were quantified by counting the number of vesicles per 2 μm^2 microscopic field in 4 randomly selected fields ($n = 4$ per group). Blue arrow: lipid droplet; green arrow: mitochondria. (E) Proposed mechanism for the anti-obesity effect of *G. cambogia* extract in adipose tissue. ** $p < 0.01$ vs. ND-fed mice, # $p < 0.05$ and ## $p < 0.01$ vs. HFD-fed mice. n.s.: not significant. The data are the mean \pm S.D.

proteins in eWAT and iWAT were observed (Figure 10A). However, HFD and *G. cambogia* administration did not affect *Klf3* transcription, unlike other target genes (Figure 10B), and correlations among the transcripts of *Klf3*, *Lc3* and *Sqstm1* could not be determined, indicating that *G. cambogia*-mediated KLF3 regulation was due to selective autophagic degradation (Figure 10C). In addition, ultrastructural findings showed that significant increases in double-membrane autophagosomes were observed in HFD-induced eWAT and iWAT, whereas in eWAT and iWAT from *G. cambogia* extract-administered mice, fewer of these features were observed by transmission electron microscopy (TEM) (Figure 10D).

Finally, we examined the effect of hydroxycitric acid (HCA, 60, 120, 180 µg/ml) at concentrations equivalent to those of *G. cambogia* extract (100, 200 and 300 µg/ml) as well as 240 µg/ml HCA on RPS6KA1, STAT3, and CEBPs expression and autophagy activation in 3T3-L1 differentiated cells (Fig. S10). We found that HCA significantly inhibited RPS6KA1 and STAT3 phosphorylation at 15 min and 2 h and CEBPB expression at 48 h in MDI-induced 3T3-L1 preadipocytes (Fig. S10A and B). In addition, HCA inhibited LC3-I and LC3-II expression and increased SQSTM1 and KLF3 expression after 72 h of stimulation (Fig. S10C). Moreover, HCA inhibited CEBPA and PPARG expression in mature 3T3-L1 adipocytes (fully differentiated adipocytes) (Fig. S10D). These results indicated that the underlying effects of *G. cambogia* extract are due, at least in part, to HCA.

Taken together, our results support the conclusion that RPS6KA1 and STAT3 activation in obese models increased autophagic activity, which contributed to SQSTM1-mediated selective degradation of KLF3 in eWAT and iWAT, and *G. cambogia* extract efficiently suppressed these processes by inhibiting RPS6KA1 and STAT3 activation (Figure 10E).

Discussion

In addition to antiobesity drugs, herbal weight-reducing agents have been used worldwide [58,59]. *G. cambogia*, one of the natural products, has been used as a weight-loss supplement in many countries, although the mechanisms are poorly understood [24–26].

In the present study, we demonstrated for the first time that (1) *G. cambogia* extract suppressed CEBPB expression by regulating its transcription in 3T3-L1 differentiated cells; (2) *G. cambogia* extract inhibited SQSTM1-mediated selective autophagic degradation of KLF3 by suppressing autophagic flux and increased KLF3-CTBP2 complex affecting *Cebpa* and *Pparg* transcription in 3T3-L1 differentiated cells; and (3) RPS6KA1 and STAT3 inhibition via *G. cambogia* extract is critical for CEBPB and autophagy regulation. These findings demonstrate key roles of RPS6KA1 and STAT3 in adipogenesis and are summarized in Figure 10E.

RPS6KA1 and STAT3, which act as important regulators by phosphorylation and nuclear translocation [60,61], are reported targets of *G. cambogia* extract [31]. Although RPS6KA1 and STAT3 did not exhibit cross-talk interaction with the treatment of specific inhibitors, siRNAs and STRING data (Figures 1A, 2C and S2A), CEBPB was affected by

G. cambogia extract, specific inhibitors and siRNA-mediated *Rps6ka1* and *Stat3* inhibition (Figure 2A–D, S2C). Since RPS6KA1-CREB and STAT3 phosphorylation regulate *Cebpb* promoter activity, we examined the *Cebpb* transcript level and found that *G. cambogia* extract suppressed *Cebpb* transcription (Figure 2F).

Autophagy regulates cell homeostasis. Although autophagy is dysregulated in diverse diseases, including obesity [62], pharmacological agents and the mechanism underlying autophagy regulation are not completely clear. The second significant finding of this study is that *G. cambogia* extract suppressed autophagic flux through autophagy-related gene regulation during differentiation (Figure 3C–E). In particular, it was reported that the intracellular level of SQSTM1 is regulated by the balance between transcriptional regulation (incoming flux) and posttranslational regulation through autophagic degradation (outcoming flux) [63]. In addition, reduced levels of SQSTM1 were detected in the adipose tissue of obese people [64], and loss of SQSTM1 in adipose tissue in mice results in obesity by upregulating *Pparg* transcription [65]. Our results showed that the level of the *Sqstm1* transcript was downregulated at day 3–4 of adipocyte differentiation and that *G. cambogia* treatment increased *Sqstm1* transcription to intensity incoming flux, which might provide more chance to interact with KLF3 as a cargo protein. Although the *Sqstm1* transcript level in control group was increased and was not significantly different from *G. cambogia* extract treated group at day 6, the SQSTM1 protein level was increased by *G. cambogia* extract compared to the control at day 6 (Figure 3A). This might be due to the inhibition of autophagic flux by *G. cambogia* extract (outcoming flux).

Since autophagy is one of the main processes by which intracellular proteins are degraded, we hypothesized that *G. cambogia* extract inhibited autophagy and adipogenesis by regulating the degradation of negative regulators. In addition, *G. cambogia* extract, FMK and stattic inhibited CEBPB expression at 72 or 96 h of treatment, and it did not appear to be sufficient to suppress CEBPA and PPARG levels, implying involvement of the CEBPB-independent regulatory signaling pathway (Figure 5B and C). Thus, we examined the levels of KLF2 and KLF3, which are well-characterized negative regulators of PPARG and CEBPA, and found that only KLF3 was increased by *G. cambogia* extract through an increase in the KLF3 protein half-life due to autophagy inhibition (Figure 5A, B,F,G and S5). Since interaction of SQSTM1 with cargo protein is necessary for selective autophagy [46], we examined the SQSTM1 level physically interacting with increased KLF3 and found that *G. cambogia* extract, FMK and stattic maintained interaction of SQSTM1 with KLF3 (Figure 6A). Interestingly, as shown in results from experiments using *Sqstm1* knock-down (Figure 6B–D), *G. cambogia* extract inhibited SQSTM1-mediated selective autophagic degradation of KLF3 without affecting SQSTM1-KLF3 interaction.

Finally, we provide the first evidence that RPS6KA1 and STAT3 act as regulators of autophagy in adipocyte differentiation. Although STAT3 is known to be a regulator of autophagy [49,60], this study might be the first observation to investigate its underlying mechanism. Interestingly, increased

KLF3 by RPS6KA1 and STAT3 inhibition interacted with CTBP2 to form a transcriptional repressor complex. Thus, regulation of *Cebpb* transcription and KLF3-CTBP2 complex formation can be important mechanisms of *G. cambogia* extract-mediated *Cebpa* and *Pparg* transcription regulation (Figures 2F, 7C-E).

However, our study had several limitations. It is well known that the decrease in body weight gain can be caused not only by a decrease in food intake but also an increase in energy expenditure. Although we did not examine energy expenditure and activity in obese mice administered *G. cambogia* extract, it has been reported that *G. cambogia* extract could enhance energy expenditure in rats [66], and no significant change in food intake was found among the animal groups in this study (Fig. S8A and B). These findings provide indirect evidence showing that supplementation with *G. cambogia* extract affects the efficiency of using food energy for the accretion of body mass, which suggests that energy expenditure is increased and that this effect as well as regulation of lipogenic gene might, at least in part, inhibit adipogenesis. Second, adipogenic differentiation using insulin induces IRS (insulin receptor substrate)-AKT/PKB (AKT serine/threonine kinase) activation and results in MTOR (mechanistic target of rapamycin kinase)-mediated autophagy inhibition [67]. Although MDI decreased LC3 level and increased KLF3 level until day 1 after starting differentiation via autophagy inhibition (Figures 3A and 5A), *G. cambogia* extract significantly attenuated autophagic flux and enhanced KLF3 expression from day 3 after starting differentiation to inhibit CEBPA and PPARG expression and suppressed adipogenesis *in vitro* and *in vivo* studies.

In conclusion, this study demonstrated that *G. cambogia* extract inhibits adipogenesis by affecting CEBPB and autophagy via *Cebpb* and autophagy-related gene regulation. In addition, *G. cambogia* extract increased KLF3 level by inhibiting SQSTM1-mediated selective autophagic degradation and enhanced the formation of KLF3-CTBP2 transcriptional complex. Moreover, we discovered that two target molecules, RPS6KA1 and STAT3, play important roles in the regulation of CEBPB and autophagy in adipocyte differentiation. These findings provide new insight into the mechanism by which *G. cambogia* suppresses adipogenesis and molecular links to therapeutic targets for the treatment of obesity.

Materials and methods

Reagents, chemicals, and antibodies

Dulbecco's modified Eagle's medium (DMEM; 11995-065), bovine calf serum (16170-078), fetal bovine serum (FBS; 16000-044), phosphate-buffered saline (PBS; 70011-044), penicillin/streptomycin, and trypsin-ethylenediaminetetraacetic acid (EDTA; 25200-072) were obtained from Gibco, Inc. (Thermo Fisher Scientific). 3-Isobutyl-1-methylxanthine (IBMX; I7018), dexamethasone (D2915), insulin (I9278), (-)-epigallocatechin gallate (EGCG; E4143), Oil red O (O0625), isopropanol (I9516), stastic (S7947), cycloheximide (CHX; C7698), bafilomycin A₁ (Baf; 5.08409), anti-rabbit-FITC (F0382), and anti-mouse-

tetramethylrhodamine (T7782) were purchased from Sigma-Aldrich. Anti-PPARG (2443), anti-CEBPA (8178), anti-phospho-RPS6KA1 (Ser380; 9341), anti-RPS6KA1 (8408), anti-phospho-STAT3 (Tyr705; 9145), anti-STAT3 (9132), anti-phospho-CREB (Ser133, 9198), anti-CREB (9197), anti-BECN1 (3495), anti-ATG7 (8558), anti-ATG3 (3415), anti-MAP1LC3/LC3 (12741), anti-ATG4B (13507), anti-ATG12 (4180), anti-CTBP1 (8684), anti-CTBP2 (13256) and anti-rabbit (7074) were purchased from Cell Signaling Technology. Anti-CEBPB (sc-7962), anti-CEBPD (sc-515028), anti-SQSTM1 (sc-48402) and anti-KLF3 (sc-514500) were purchased from Santa Cruz Biotechnology. Anti-KLF2 (NB100-1051) was purchased from Novus Biologicals. Anti-ACTB (LF-PA0207) and goat anti-mouse (LF-SA8001) antibodies were purchased from Abfrontier. Normal rabbit IgG (I-1000) and normal mouse IgG (I-2000) were purchased from Vector Laboratories. *Garcinia cambogia* extract powder (main component: hydroxycitric acid, 59.55%) was obtained from Mirae Biotech, Inc. (130219) according to a previous study [31]. 1-(4-Amino-7-(3-hydroxypropyl)-5-p-tolyl-7 H-pyrrolo[2,3-d]pyrimidin-6-yl)-2-fluoroethanone (FMK) was purchased from Axon Medchem (1848). LY294002 (LY; 70820), 3-methyladenine (3-MA; 13242) and rapamycin (Ra; 13346) were purchased from Cayman Chemical. MG132 was purchased from AG Scientific, Inc (M-1157). All other chemicals were analytical grade.

Cell culture

Cell culture was performed as previously described [31]. Mouse 3T3-L1 preadipocytes were obtained from the American Type Culture Collection (ATCC CL-173™) and grown in DMEM supplemented with 10% (v:v) heat-inactivated bovine calf serum, 100 IU/ml penicillin, and 100 µg/ml streptomycin at 37°C in a humidified incubator under 95% air and 5% CO₂. 3T3-L1 cells were used at passages 6–8. Cells were seeded on different types of dishes according to each assay. For differentiation, 3T3-L1 preadipocytes were cultured in MDI (DMEM containing 0.5 mM isobutylmethylxanthine [IBMX], 5 µM dexamethasone, 0.5 µg/ml insulin and 10% FBS) medium for 2 days. Next, the medium was replaced with DMEM containing 10% FBS and 5 µg/ml insulin (IF medium). After 48 h, the medium was replaced with DMEM containing 10% FBS and was replaced once more for 48 h. The *G. cambogia* extract (dissolved in D. W.) and other reagents (dissolved in DMSO; final DMSO concentration in medium was ≤ 0.2%) were added when the media was replaced for the indicated time periods.

Oil red O staining

Oil red O staining for lipid droplets was performed as previously described [31]. Mature 3T3-L1 adipocytes were stained with Oil red O after 8 days of differentiation. The cells were fixed for 1 h at room temperature using 4% formaldehyde and washed with 60% isopropanol. Next, the fixed cells were stained with filtered Oil red O solution in 60% isopropanol for 10 min. After the Oil red O solution was removed, the stained cells were washed with water. Images

of lipid droplets in the stained cells were photographed using an Olympus IX71 digital microscope (Olympus, Tokyo, Japan). Then, the stained lipid droplets were dissolved in 100% isopropanol and quantified by measuring the absorbance at 520 nm using a microplate reader (Tecan Group Ltd., Männedorf, Switzerland).

LDH (lactate dehydrogenase) release assay

3T3-L1 preadipocytes were seeded in 96-well plates. After 24 h, *G. cambogia* extract (100, 200 and 300 µg/ml) and lysis buffer (positive control) were added to the cells. After 48 or 72 h of incubation, the LDH assay was performed using Quanti-LDH™ Cytotoxicity Assay Kit (BioMAX Co., BCT-LDH) according to the manufacturer's instructions. The absorbance was measured using a microplate reader (Tecan Group Ltd.). The data are presented as the percentage of LDH released into the medium as a control (without treatment) to 100%.

Kinase assay

The *in vitro* MAPK3/ERK1 kinase assay was carried out in accordance with the instructions provided by the MAPK3/ERK1 Kinase Enzyme System and ADP-Glo™ Kinase Assay (Promega, V9281). The JAK2 kinase assay was performed using active JAK2 enzyme, protein tyrosine kinase substrate (poly-Glu,Tyr 4:1) (BPS Bioscience, 79520) and the ADP-Glo™ Kinase Assay according to the manufacturer's instructions. In brief, *G. cambogia* extract was incubated with active MAPK3/ERK1 or JAK2 enzyme with each substrate and ATP solution in the assay buffer for 1 h. The MAPK3/ERK1 and JAK2 kinase assay mixtures were incubated with ADP-Glo™ reagent for 40 min, and kinase detection reagent was added for 30 min. After finishing the reaction, the luminescence was determined with a GloMax 20/20 luminometer reader (Promega, Madison, WI, USA). Specific kinase activity was expressed as the relative activity ratio of the control group.

Integration of protein-protein interaction (PPI) analysis

Using the search tool for retrieval of interacting genes/proteins database (STRING, <http://string-db.org/>) [68], which integrates both known and predicted PPIs, we constructed a network associated with RPS6KA1 and STAT3. Active interaction sources, including text mining, experiments, databases, coexpression, neighborhood, gene fusion and cooccurrence, as well as limiting the species to "Homo sapiens" and an interaction score > 0.4, were applied to construct the PPI networks.

Western blot analysis

Western blotting was performed to detect protein levels in cells or tissues. Proteins from cells or tissues were extracted in ice-cold RIPA buffer (50 mM Tris-HCl, pH 8.0, 150 mM NaCl, 1.0% NP-40 [Sigma-Aldrich, I8896], 2 mM EDTA [Sigma-Aldrich, E9884], 5 mM NaF [Sigma-Aldrich, S7920], 1 mM phenylmethylsulfonyl fluoride [PMSF; Sigma-Aldrich, P7626], 1 mM sodium orthovanadate [Sigma-Aldrich, S6508], 0.5% sodium

deoxycholate [Sigma-Aldrich, D6750]; and 0.1% sodium dodecyl sulfate [SDS; Wako, 191-07145]). The protein concentration of the lysates was quantified using a BCA protein assay kit (Pierce, 23225). Equivalent amounts of protein were separated using sodium dodecyl sulfate-polyacrylamide gel electrophoresis (SDS-PAGE, 10–15%) and transferred to polyvinylidene fluoride (PVDF) membranes (ATTO Corp., AE-6667-p). The membranes were blocked with TBS-T (10 mM Tris, 150 mM NaCl, 0.1% Tween-20 [Duchefa Biochemie, P1362.0500], pH 7.6) containing 5% bovine serum albumin (BSA, Bovogen, BSAS-AU) for 1 h. The membranes were incubated with primary antibodies overnight and then incubated with secondary antibodies for 6 h at 4°C. Specific signals were detected using an enhanced chemiluminescence reagent (ATTO Corp., WSE-7120 L). The band densities were quantified using Image Lab software (Version 5.2.1, Bio-Rad, Hercules, CA, USA).

Quantitative real-time PCR (qPCR)

After the differentiation of 3T3-L1 preadipocytes in the presence or absence of several reagents for the indicated times, total RNA was isolated using TRIzol reagent (Invitrogen, 15596-018) according to the manufacturer's instructions. In addition, total RNA from adipose tissues was extracted using TRIzol reagent. Reverse transcription was performed using the AccuPower CycleScript RT Premix kit (Bioneer, K-2045) by incubating the complete reaction mix and 1 µg of RNA in a thermocycler. Real-time PCR amplification was performed using SYBR Green qPCR Premix (Toyobo, QPK-201) and 96-well optical plates in a CFX96 real-time detection system (Bio-Rad) under the following conditions: 1 cycle of 95°C for 3 min; 39 cycles of 95°C for 10 s and 60°C for 30 s; and 1 cycle of 95°C for 10 s and 65°C for 5 s, followed by 0.5°C increments at 5 s/step to 95°C. Only primer pairs leading to the synthesis of a single fragment with the appropriate size were used in this study. The primer sets used for this study are listed in Table S1. Relative gene expression levels were calculated using the $2^{-\Delta\Delta Ct}$ method and normalized to *Actb* expression levels.

Protein half-life analysis

The half-life of the CEBPB and KLF3 proteins was measured by the CHX chase assay. For CEBPB protein, 3T3-L1 preadipocytes were incubated with MDI medium for 42 h in the presence or absence of *G. cambogia* extract. Then, the cells were treated with CHX (1.5 µg/ml) for the indicated times (0, 2, 4 and 6 h) and harvested for western blot analysis. For KLF3 protein, 3T3-L1 preadipocytes were incubated with MDI medium for 48 h, followed by IF medium for 8 h in the presence or absence of *G. cambogia* extract. Then, cells were treated with CHX (1.5 µg/ml) during IF medium incubation for the indicated times (0, 4, 8 and 16 h) and harvested for western blot analysis.

Plasmid construction and lentivirus production

FUW mCherry-green fluorescent protein (GFP)-LC3 was a gift from Anne Brunet (Addgene, 110060; <http://n2t.net/>)

addgene:110060; RRID:Addgene_110060) [69]. The lentiviral packaging plasmids, pMD2.G and psPAX2 were gifts from Didier Trono (Addgene, 12259; <http://n2t.net/addgene:12259>; RRID:Addgene_12259, and 12260; <http://n2t.net/addgene:12260>; RRID:Addgene_12260). Those were cotransfected with the genomic plasmid into HEK293T cells (ATCC CRL-3216TM) using iNfect (iNtRON Biotechnology Inc., 15,081) to produce recombinant viral particles. After 48 h, virus-containing medium was collected and the virus titers were measured using Lenti-X p24 rapid titer kit (Takara Bio Inc, 632200).

Measurement of autophagic flux

Autophagic flux was measured in mCherry-GFP-LC3-transfected 3T3-L1 differentiated cells using an imaging-based assay. 3T3-L1 preadipocytes were transfected with mCherry-GFP-LC3 lentiviruses at a multiplicity of infection (MOI) of 40 with 8 µg/ml polybrene (Sigma-Aldrich, H9268). After 24 h, cell differentiation was performed with *G. cambogia* extract. After 48 h of differentiation incubating MDI medium, LY294002 (10 µM), 3-MA (0.5 mM), bafilomycin A₁ (100 nM) and rapamycin (10 nM) were added to IF medium for 24 h. The images of mCherry-GFP-LC3 were captured with a confocal laser microscope (Nanoscope Systems, Daejeon, Korea), and the numbers of yellow (autophagosome, mCherry + GFP-LC3 puncta) and red (autolysosome, loss of GFP fluorescence in acidic environment, mCherry + GFP-LC3 puncta was observed as a decrease in yellow puncta) puncta were counted to determine the extent of the autophagic flux.

For immunoblotting, 3T3-L1 preadipocytes were differentiated with *G. cambogia* extract. After 48 h of differentiation incubating MDI medium, LY294002 (10 µM), 3-MA (0.5 mM), bafilomycin A₁ (100 nM) and rapamycin (10 nM) were added to IF medium for 24 h. After finishing the treatment, proteins from cells were collected by western blot analysis

Small-interfering RNA transfection

Duplex siRNAs targeting *Rps6ka1* (accession no. NM_001285505.1, 20 nM), *Stat3* (accession no. NM_011486.5, 30 nM), *Cebpb* (accession no. NM_001287738.1, 10 nM), *Sqstm1* (accession no. NM_001287738.1, 30 nM) and scramble siRNA (siCon, SN-1003) were purchased from Bioneer Inc. (Daejeon, Korea). 3T3-L1 preadipocytes were transfected with siRNAs using Lipofectamine 2000 (Invitrogen, 11668019) in Opti-MEM (Thermo Fisher, 31985-070) for 4 h according to the manufacturer's protocol. Then, the cells were differentiated for 72 h by incubation in differentiation medium (48 h for MDI and 24 h for IF medium). The ability of the duplex siRNA to knock down target gene expression was analyzed by qPCR and western blotting. The sequences of the siRNAs used are listed in Table S2.

Immunoprecipitation assay

Immunoprecipitation assay was performed to detect the interaction of KLF3 with the SQSTM1, CTBP1 and CTBP2

proteins. 3T3-L1 preadipocytes were treated with *G. cambogia* extract, FMK and statin for 72 h in differentiation medium (48 h for MDI and 24 h for IF medium). Then, the cells were washed with cold PBS and lysed in ice-cold RIPA buffer (50 mM Tris-HCl, pH 8.0, 150 mM NaCl, 1.0% NP-40, 2 mM EDTA, 5 mM NaF, 1 mM PMSF, 1 mM sodium orthovanadate, 0.5% sodium deoxycholate, and 0.1% sodium dodecyl sulfate). After centrifugation, 500 µg of cell lysate was incubated with 1 µg of the KLF3 antibody at 4°C overnight. The lysate immunoprecipitated with anti-IgG served as a negative control. The immune complexes were then purified with 30 µl of protein A magnetic beads (Pureproteome; Millipore, LSKMAGA10) at 4°C for 4 h, centrifuged and washed with PBS with 0.1% Tween-20. The immunoprecipitated proteins were further analyzed by western blotting.

Animals and diet

Four-week-old male C57BL/6 N mice (21–23 g) were obtained from Orient Bio Inc. (Seongnam, Korea). The animals were housed two per cage and provided normal chow and water ad libitum in the animal facility under controlled temperature (22 ± 2°C), humidity (50 ± 5%), and lighting (12/12 h dark-light cycle, lights on at 7:00 a.m.) conditions. After a 1-week acclimatization period, animal experiments were performed according to procedures approved by the Institutional Animal Care and Use Committee of Chungnam National University (CNU-01147) and The ARRIVE (Animal Research: Reporting of In Vivo Experiments) guidelines [70].

For the obese mouse model, mice were randomly divided into five groups (n = 8 in each group): normal diet (ND, control), high-fat diet (HFD), HFD + 200 mg/kg *G. cambogia* extract (HFD + Ga 200), HFD + 400 mg/kg *G. cambogia* extract (HFD + Ga 400) and HFD + 20 mg/kg orlistat (HFD + Orli 20, positive control). The control group mice were fed a ND (10% kcal from fat; Research Diets, Inc., R12450B), and the HFD group mice were fed a high-fat diet (40% kcal from fat; Research Diets, Inc., R12079B) ad libitum with free access to water for 8 weeks. Mice were administered *G. cambogia* extract or orlistat dissolved in 0.5% carboxymethyl cellulose (CMC, Sigma-Aldrich, C5678) orally every day. Body weight and food intake were recorded twice per week. To calculate the caloric intake, the consumed food in grams was multiplied by the calories per gram of the respective type of food (ND: 3.82 Kcal/g; HFD: 4.67 Kcal/g). The energy efficiency rate was calculated by dividing body weight gain by caloric intake [71]. At the end of the experimental period, all animals were fasted for 12 h, anaesthetized by CO₂ administration, and photographed. After the mice were euthanized by cervical dislocation, tissues were collected, rinsed, photographed, weighed, and directly stored at -80°C until further analysis.

Serum analysis and tissue isolation

After 8 weeks of feeding, the mice were put under deep anesthesia with CO₂ after overnight fasting. Before tissue harvest, blood samples were collected from the abdominal aorta and centrifuged at 4,000 x g for 20 min to separate the supernatant, which was designated serum. Triglyceride, total

cholesterol, GPT/ALT (glutamic pyruvic transaminase, soluble) and GOT1/AST (glutamic-oxaloacetic transaminase 1, soluble) levels were analyzed using a DRI-CHEM 7000i (Fuji Film, Tokyo, Japan). The weights of the fat tissues (epididymal white [eWAT], mesenteric white [mWAT], retroperitoneal white [rWAT], inguinal subcutaneous white [iWAT], and brown fat) were also measured.

Histological analysis

Epididymal and inguinal subcutaneous white adipose tissues and liver were fixed with 4% paraformaldehyde, dehydrated, and embedded in optimal cutting temperature (O.C.T.) compound (Sakura, 4583). The tissues were cut into 10- μ m-thick sections. The sections were stained with hematoxylin and eosin (H&E) for histological examination of lipid droplets, and images were acquired using a microscope (Nikon Eclipse Ti, Nikon Instruments Inc., Tokyo, Japan). The distribution of adipocyte size was determined using ImageJ software (Adiposoft V1.16; NIH, Bethesda, MD, USA) [72]. Heart, spleen, lung and kidney tissues were fixed with 4% paraformaldehyde and embedded in paraffin. The tissues were cut into 4- μ m-thick sections and sections were stained with H&E for histological examination. The scale bars of the images represent 50 μ m.

Glucose homeostasis examination

The oral glucose tolerance test (OGTT) was performed as previously described [73]. The animals were fasted overnight, and blood glucose levels were measured using an Accu-Chek Active blood glucose meter (Roche Diagnostics, Rotkreuz, Switzerland) at 0, 15, 30, 45, 60, 90, 120 and 150 min after oral glucose loading (2 g/kg). The insulin tolerance test (ITT) followed the same protocol as the OGTT, except for the intraperitoneal administration of insulin (0.75 U/kg) after glucose administration.

Immunofluorescence assay

Dual immunofluorescence was performed in 3T3-L1 differentiated cells and sections of eWAT and iWAT. For cell analysis, coverslips were placed inside 24-well plates, and cells were seeded on coverslips. After the differentiation of cells in the presence or absence of several reagents for 72 h (48 h for MDI and 24 h for IF medium), the cells were fixed with 4% formaldehyde and permeabilized with 0.25% Triton X-100 (Sigma-Aldrich, T9284) in PBS with 1% BSA for 5 min. Then, the cells were blocked with 5% goat serum (Vector, S-1000) in PBS. After 1 h, the cells were incubated with LC3 and KLF3 or KLF3 and CTBP2 antibodies for 18 h at 4°C, and secondary antibodies (FITC and TRITC) in 3% BSA were added and incubated for 2.5 h at room temperature. Then, the nuclei were stained with 4',6-diamidino-2-phenylindole (DAPI, Vector, H-1200), and the cells were observed under a confocal laser microscope (K1-Fluo, Nanoscope systems, Daejeon, Korea) using K1-image software (Nanoscope systems). The numbers of yellow dot (FITC for LC3 + TRITC for KLF3) were counted to determine the extent of the sequestration of KLF3 to LC3. The colocalization of KLF3 and

CTBP2 was quantified using ImageJ software (Version 1.52p, NIH, Bethesda, MD, USA) and assessed by using the Pearson correlation coefficient [74,75].

Dissected eWAT and iWAT (10 μ m) were stained with p-RPS6KA1 (Ser380), p-STAT3 (Tyr705) and KLF3 antibodies, followed by secondary antibodies (FITC and TRITC). Normal isotype IgG was used as a negative control. The images were captured with a confocal laser microscope (Nanoscope systems, Daejeon, Korea). The scale bars of the images represent 50 μ m. The fluorescence intensities of green and red (indicating LC3 and KLF3, respectively) were assessed using ImageJ software.

Transmission electron microscopy (TEM) analysis

d fixed with 2.5% glutaraldehyde in 0.1 M cacodylate buffer (pH 7.3). After fixation, the tissues were treated with 4% osmium tetroxide (OsO₄, Electron Microscopy Sciences, 19190) plus 3% potassium ferrocyanide (Sigma-Aldrich, P9387) in 0.1 M cacodylate buffer (pH 7.3, Electron Microscopy Sciences, 12300) for 1 h at 4°C in the dark and embedded in Epon 812 (Electron Microscopy Sciences, 14120) after dehydration in an ethanol and propylene oxide series. Polymerization was conducted using pure resin at 70°C for two days. Ultrathin sections (70 nm) were obtained with an EM UC7 ultramicrotome (Leica, Vienna, Austria), which were then collected on 150 mesh copper grids (Electron Microscopy Sciences, G150-Cu). The sections were stained with 2% uranyl acetate (Electron Microscopy Sciences, 22400) for 10 min and lead citrate for 5 min. The stained sections were scanned at 120 kV using a Tecnai G2 Spirit Twin transmission electron microscope (FEI Company, Hillsboro, OR, USA).

Statistical analyses

All data are expressed as the mean \pm S.D. of at least 3–5 independent experiments. Statistical analyses were performed with GraphPad Prism software (Version 9, San Diego, CA, USA). A two-sided, unpaired Student's t-test was used to analyze the difference between two groups of data with normally distributed variables. The Mann-Whitney test was used to analyze nonnormally distributed variables. Differences among three or more groups were analyzed with one-way analysis of variance (ANOVA) followed by a post hoc Bonferroni test. The correlations between p-RPS6KA1, p-STAT3, LC3, SQSTM1 and KLF3 in the western blot data or *Lc3*, *Sqstm1* and *Klf3* in the transcript data were determined by Pearson's rank test. Differences with $p < 0.05$ were considered statistically significant.

Acknowledgments

We are grateful to Korea Basic Science Institute for valuable support in the cryo-TEM measurements using ultramicrotome and bio-TEM instruments.

Disclosure of potential conflicts of interest

The authors declare that they have no conflict of interest.

Funding

This study was supported by National Research Foundation of Korea (NRF) grant funded by the Korean government (No. 2019R1C1C1010698).

ORCID

Joo-Hui Han  <http://orcid.org/0000-0002-3638-0581>

Chang-Seon Myung  <http://orcid.org/0000-0002-6292-2911>

References

- [1] Rosen ED, Spiegelman BM. Adipocytes as regulators of energy balance and glucose homeostasis. *Nature*. 2006;444:847–853.
- [2] Luo L, Liu M. Adipose tissue in control of metabolism. *J Endocrinol*. 2016;231:R77–R99.
- [3] Bhupathiraju SN, Hu FB. Epidemiology of obesity and diabetes and their cardiovascular complications. *Circ Res*. 2016;118:1723–1735.
- [4] Cercato C, Fonseca FA. Cardiovascular risk and obesity. *Diabetol Metab Syndr*. 2019;11:74.
- [5] Farmer SR. Transcriptional control of adipocyte formation. *Cell Metab*. 2006;4:263–273.
- [6] Lowe CE, O'Rahilly S, Rochford JJ. Adipogenesis at a glance. *J Cell Sci*. 2011;124:2681–2686.
- [7] Rangwala SM, Lazar MA. Transcriptional control of adipogenesis. *Annu Rev Nutr*. 2000;20:535–559.
- [8] Guo L, Li X, Tang QQ. Transcriptional regulation of adipocyte differentiation: a central role for CCAAT/enhancer-binding protein (C/EBP) beta. *J Biol Chem*. 2015;290:755–761.
- [9] Rosen E, Eguchi J, Xu Z. Transcriptional targets in adipocyte biology. *Expert Opin Ther Targets*. 2009;13:975–986.
- [10] Lee JE, Ge K. Transcriptional and epigenetic regulation of PPARgamma expression during adipogenesis. *Cell Biosci*. 2014;4:29.
- [11] Wu Z, Wang S. Role of kruppel-like transcription factors in adipogenesis. *Dev Biol*. 2013;373:235–243.
- [12] Ross SE, Hemati N, Longo KA, et al. Inhibition of adipogenesis by Wnt signaling. *Science*. 2000;289:950–953.
- [13] Hudak CS, Sul HS. Pref-1, a gatekeeper of adipogenesis. *Front Endocrinol (Lausanne)*. 2013;4:79.
- [14] Banerjee SS, Feinberg MW, Watanabe M, et al. The Kruppel-like factor KLF2 inhibits peroxisome proliferator-activated receptor-gamma expression and adipogenesis. *J Biol Chem*. 2003;278:2581–2584.
- [15] Sue N, Jack BH, Eaton SA, et al. Targeted disruption of the basic Kruppel-like factor gene (Klf3) reveals a role in adipogenesis. *Mol Cell Biol*. 2008;28:3967–3978.
- [16] Turner J, Crossley M. Cloning and characterization of mCtBP2, a co-repressor that associates with basic Kruppel-like factor and other mammalian transcriptional regulators. *EMBO J*. 1998;17:5129–5140.
- [17] Klionsky DJ, Emr SD. Autophagy as a regulated pathway of cellular degradation. *Science*. 2000;290:1717–1721.
- [18] Wesselborg S, Stork B. Autophagy signal transduction by ATG proteins: from hierarchies to networks. *Cell Mol Life Sci*. 2015;72:4721–4757.
- [19] Zhang Y, Sowers JR, Ren J. Targeting autophagy in obesity: from pathophysiology to management. *Nat Rev Endocrinol*. 2018;14:356–376.
- [20] Clemente-Postigo M, Tinahones A, El Bekay R, et al. The role of autophagy in white adipose tissue function: implications for metabolic health. *Metabolites*. 2020;10(5):179.
- [21] Li H, Yuan Y, Zhang Y, et al. Icarin inhibits AMPK-dependent autophagy and adipogenesis in adipocytes in vitro and in a model of graves' orbitopathy in vivo. *Front Physiol*. 2017;8:45.
- [22] Singh R, Xiang Y, Wang Y, et al. Autophagy regulates adipose mass and differentiation in mice. *J Clin Invest*. 2009;119:3329–3339.
- [23] Zhang Y, Goldman S, Baerga R, et al. Adipose-specific deletion of autophagy-related gene 7 (atg7) in mice reveals a role in adipogenesis. *Proc Natl Acad Sci U S A*. 2009;106:19860–19865.
- [24] Semwal RB, Semwal DK, Vermaak I, et al. A comprehensive scientific overview of *Garcinia cambogia*. *Fitoterapia*. 2015;102:134–148.
- [25] Marquez F, Babio N, Bullo M, et al. Evaluation of the safety and efficacy of hydroxycitric acid or *Garcinia cambogia* extracts in humans. *Crit Rev Food Sci Nutr*. 2012;52:585–594.
- [26] Chong PW, Beah ZM, Grube B, et al. IQP-GC-101 reduces body weight and body fat mass: a randomized, double-blind, placebo-controlled study. *Phytother Res*. 2014;28:1520–1526.
- [27] Kim KY, Lee HN, Kim YJ, et al. *Garcinia cambogia* extract ameliorates visceral adiposity in C57BL/6J mice fed on a high-fat diet. *Biosci Biotechnol Biochem*. 2008;72:1772–1780.
- [28] Bilal T, Gursel FE, Ates A, et al. Effect of *Garcinia cambogia* extract on body weight gain, feed intake and feed conversion ratio, and serum non-esterified fatty acids and C-reactive protein levels in rats fed with atherogenic diet. *Iran J Vet Res*. 2012;13:330–333.
- [29] Blenis J. Signal transduction via the MAP kinases: proceed at your own RSK. *Proc Natl Acad Sci U S A*. 1993;90:5889–5892.
- [30] Levy DE, Darnell JE Jr. Stats: transcriptional control and biological impact. *Nat Rev Mol Cell Biol*. 2002;3:651–662.
- [31] Han JH, Jang KW, Park MH, et al. *Garcinia cambogia* suppresses adipogenesis in 3T3-L1 cells by inhibiting p90RSK and Stat3 activation during mitotic clonal expansion. *J Cell Physiol*. 2021;236:1822–1839.
- [32] Rosen ED, Hsu CH, Wang X, et al. C/EBPalpha induces adipogenesis through PPARgamma: a unified pathway. *Genes Dev*. 2002;16:22–26.
- [33] Lefterova MI, Lazar MA. New developments in adipogenesis. *Trends Endocrinol Metab*. 2009;20:107–114.
- [34] Descombes P, Schibler U. A liver-enriched transcriptional activator protein, LAP, and a transcriptional inhibitory protein, LIP, are translated from the same mRNA. *Cell*. 1991;67:569–579.
- [35] Yu HS, Kim WJ, Bae WY, et al. *Inula britannica* inhibits adipogenesis of 3T3-L1 preadipocytes via modulation of mitotic clonal expansion involving ERK 1/2 and Akt signaling pathways. *Nutrients*. 2020;12:3037.
- [36] Deng J, Hua K, Lesser SS, et al. Activation of signal transducer and activator of transcription-3 during proliferative phases of 3T3-L1 adipogenesis. *Endocrinology*. 2000;141:2370–2376.
- [37] Zhang K, Guo W, Yang Y, et al. JAK2/STAT3 pathway is involved in the early stage of adipogenesis through regulating C/EBPbeta transcription. *J Cell Biochem*. 2011;112:488–497.
- [38] Boglari G, Szeberenyi J. Nuclear translocation of p90Rsk and phosphorylation of CREB is induced by ionomycin in a Ras-independent manner in PC12 cells. *Acta Biol Hung*. 2002;53:325–334.
- [39] Zhang JW, Klemm DJ, Vinson C, et al. Role of CREB in transcriptional regulation of CCAAT/enhancer-binding protein beta gene during adipogenesis. *J Biol Chem*. 2004;279:4471–4478.
- [40] Hattori T, Ohoka N, Inoue Y, et al. C/EBP family transcription factors are degraded by the proteasome but stabilized by forming dimer. *Oncogene*. 2003;22:1273–1280.
- [41] Fu DC, Lala-Tabbert N, Lee HB, et al. Mdm2 promotes myogenesis through the ubiquitination and degradation of CCAAT/enhancer-binding protein beta. *J Biol Chem*. 2015;290:10200–10207.
- [42] Yang H, Kang MJ, Hur G, et al. Sulforaphene suppresses adipocyte differentiation via induction of post-translational degradation of CCAAT/enhancer binding protein beta (C/EBPbeta). *Nutrients*. 2020;12:758.
- [43] Dong H, Czaja MJ. Regulation of lipid droplets by autophagy. *Trends Endocrinol Metab*. 2011;22:234–240.
- [44] Mizushima N, Yoshimori T, Ohsumi Y. The role of Atg proteins in autophagosome formation. *Annu Rev Cell Dev Biol*. 2011;27:107–132.

- [45] Mizushima N, Yoshimori T, Levine B. Methods in mammalian autophagy research. *Cell*. 2010;140:313–326.
- [46] Johansen T, Lamark T. Selective autophagy mediated by autophagic adapter proteins. *Autophagy*. 2011;7:279–296.
- [47] Hansen TE, Johansen T. Following autophagy step by step. *BMC Biol*. 2011;9:39.
- [48] Fullgrabe J, Ghislat G, Cho DH, et al. Transcriptional regulation of mammalian autophagy at a glance. *J Cell Sci*. 2016;129:3059–3066.
- [49] You L, Wang Z, Li H, et al. The role of STAT3 in autophagy. *Autophagy*. 2015;11:729–739.
- [50] Guo L, Huang JX, Liu Y, et al. Transactivation of Atg4b by C/EBPbeta promotes autophagy to facilitate adipogenesis. *Mol Cell Biol*. 2013;33:3180–3190.
- [51] Kraft C, Peter M, Hofmann K. Selective autophagy: ubiquitin-mediated recognition and beyond. *Nat Cell Biol*. 2010;12:836–841.
- [52] Pohl C, Dikic I. Cellular quality control by the ubiquitin-proteasome system and autophagy. *Science*. 2019;366:818–822.
- [53] Shaid S, Brandts CH, Serve H, et al. Ubiquitination and selective autophagy. *Cell Death Differ*. 2013;20:21–30.
- [54] Fajas L. Adipogenesis: a cross-talk between cell proliferation and cell differentiation. *Ann Med*. 2003;35:79–85.
- [55] Cha JY, Nepali S, Lee HY, et al. Chrysanthemum indicum L. ethanol extract reduces high-fat diet-induced obesity in mice. *Exp Ther Med*. 2018;15:5070–5076.
- [56] Attia RT, Abdel-Mottaleb Y, Abdallah DM, et al. Raspberry ketone and Garcinia Cambogia rebalanced disrupted insulin resistance and leptin signaling in rats fed high fat fructose diet. *Biomed Pharmacother*. 2019;110:500–509.
- [57] Sripradha R, Magadi SG. Efficacy of garcinia cambogia on body weight, inflammation and glucose tolerance in high fat fed male wistar rats. *J Clin Diagn Res*. 2015;9:BF01–4.
- [58] Blanck HM, Serdula MK, Gillespie C, et al. Use of nonprescription dietary supplements for weight loss is common among Americans. *J Am Diet Assoc*. 2007;107:441–447.
- [59] Pittler MH, Schmidt K, Ernst E. Adverse events of herbal food supplements for body weight reduction: systematic review. *Obes Rev*. 2005;6:93–111.
- [60] Frodin M, Gammeltoft S. Role and regulation of 90 kDa ribosomal S6 kinase (RSK) in signal transduction. *Mol Cell Endocrinol*. 1999;151:65–77.
- [61] Richard AJ, Stephens JM. The role of JAK-STAT signaling in adipose tissue function. *Biochim Biophys Acta*. 2014;1842:431–439.
- [62] Rubinsztein DC, Codogno P, Levine B. Autophagy modulation as a potential therapeutic target for diverse diseases. *Nat Rev Drug Discov*. 2012;11:709–730.
- [63] Puissant A, Fenouille N, Auberger P. When autophagy meets cancer through p62/SQSTM1. *Am J Cancer Res*. 2012;2:397–413.
- [64] Kosacka J, Kern M, Kloting N, et al. Autophagy in adipose tissue of patients with obesity and type 2 diabetes. *Mol Cell Endocrinol*. 2015;409:21–32.
- [65] Rodriguez A, Duran A, Selloum M, et al. Mature-onset obesity and insulin resistance in mice deficient in the signaling adapter p62. *Cell Metab*. 2006;3:211–222.
- [66] Vasselli J, Shane E, Boozer CN, et al. Garcinia cambogia extract inhibits body weight gain via increased energy expenditure (EE) in rats. *FASEB J*. 1998;12:A505.
- [67] Codogno P, Meijer AJ. Autophagy: a potential link between obesity and insulin resistance. *Cell Metab*. 2010;11:449–451.
- [68] Szklarczyk D, Gable AL, Lyon D, et al. STRING v11: protein-protein association networks with increased coverage, supporting functional discovery in genome-wide experimental datasets. *Nucleic Acids Res*. 2019;47:D607–D13.
- [69] Leeman DS, Hebestreit K, Ruetz T, et al. Lysosome activation clears aggregates and enhances quiescent neural stem cell activation during aging. *Science*. 2018;359:1277–1283.
- [70] Kilkenny C, Browne WJ, Cuthill IC, et al. Improving bioscience research reporting: the ARRIVE guidelines for reporting animal research. *PLoS Biol*. 2010;8:e1000412.
- [71] Winzell MS, Ahren B. The high-fat diet-fed mouse: a model for studying mechanisms and treatment of impaired glucose tolerance and type 2 diabetes. *Diabetes*. 2004;53(Suppl 3):S215–9.
- [72] Galarraga M, Campion J, Munoz-Barrutia A, et al. Adiposoft: automated software for the analysis of white adipose tissue cellularity in histological sections. *J Lipid Res*. 2012;53:2791–2796.
- [73] Han JH, Tuan NQ, Park MH, et al. Cucurbitane triterpenoids from the fruits of momordica charantia improve insulin sensitivity and glucose homeostasis in streptozotocin-induced diabetic mice. *Mol Nutr Food Res*. 2018;62:e1700769.
- [74] Dunn KW, Kamocka MM, McDonald JH. A practical guide to evaluating colocalization in biological microscopy. *Am J Physiol Cell Physiol*. 2011;300:C723–42.
- [75] Li Q, Lau A, Morris TJ, et al. A syntaxin 1, Galpha(o), and N-type calcium channel complex at a presynaptic nerve terminal: analysis by quantitative immunocolocalization. *J Neurosci*. 2004;24:4070–4081.